Investigation of Multi-Digit Tactile Integration

Investigation of Multi-Digit Tactile Integration: Evidence for Sub-Optimal Human Performance

By ROSE JAJARMI,
Hon. B.Sc.

A Thesis Submitted to the School of Graduate Studies
in the Partial Fulfillment of the Requirements for the Degree of

Masters of Science

Department of Psychology, Neuroscience & Behaviour
McMaster University
Hamilton, Ontario

Masters of Science (2023)
Department of PNB
McMaster University
Hamilton, Ontario, Canada

TITLE: Investigation of Multi-Digit Tactile Integration: Evidence for Sub-Optimal Human Performance

AUTHOR:
Rose Jajarmi,
B.Sc.

SUPERVISOR:
Daniel Goldreich
Professor, Psychology, Neuroscience & Behaviour,
McMaster University, ON, Canada

NUMBER OF PAGES: xiv, 83

Lay Abstract

This thesis investigates the neural mechanisms behind tactile perception, specifically how the brain combines multiple sensory cues to construct a unified percept when interacting with objects through touch. Typically, optimal sensory integration involves assigning more weight to more reliable cues. Our research focused on tactile integration by examining participants' ability to perceive the positions of edges crossing their index, middle, and ring fingers simultaneously. The results indicated that, contrary to predictions, participants exhibited various sub-optimal cue integration strategies. Their ability to perceive the combined positions of all three fingers was not superior to that of the best-performing individual finger. We also explored cue conflict situations, where the locations of the tactile cues were no longer from a straight edge, unbeknown to participants, and the results here reinforced the finding that participants did not consistently employ optimal cue combination strategies. This research offers valuable insights into how the brain processes tactile information.

Abstract

When examining objects using tactile senses, individuals often incorporate multiple sources of haptic sensory information to estimate the object's properties. How do our brains integrate various cues to form a single percept of the object? Previous research has indicated that integration from cues across sensory modalities is optimally achieved by weighting each cue according to its variance, such that more reliable cues have more weight in determining the percept. To explore this question in the context of a within-modality haptic setting, we assessed participants' perception of edges that cross the index, middle, and ring fingers of the right hand. We used a 2-interval forced choice (2IFC) task to measure the acuity of each digit individually, as well as the acuity of all three digits working together, by asking participants to distinguish the locations of two closely spaced plastic edges. In examining the data, we considered three perceptual models, an optimal (Bayesian) model, an unweighted average model, and a winner-take-all model. The results indicate that participants perceived sub-optimally, such that the acuity of the three digits together did not exceed that of the best individual digit. We further investigated our question by having participants unknowingly undergo a 2IFC cue conflict condition, where they thought they were touching a straight edge which was actually staggered and thus gave each digit a different positional cue. Our analyses indicate that participants did not undertake optimal cue combination but are inconclusive with respect to which suboptimal strategy they employed.

Acknowledgements

I would like to express my heartfelt gratitude to the individuals who have contributed to the completion of this thesis.

First and foremost, I am profoundly thankful to my research supervisor, Dr. Daniel Goldreich, for his guidance, mentorship, and unwavering support throughout my research journey. His guidance not only shaped the direction of this thesis but also enriched my academic experience and introduced me the world of Bayesian thinking, from which we all can benefit from.

Furthermore, I am grateful for the dedicated undergraduate lab members I had the privilege to mentor. These include students such as Ali Rezazadeh Shirazi and Aadithya Shankar, who were there with me at the start of this project. I would also extend my sincere gratitude to the valuable contributions of the undergraduate students who joined me later. These students are Kourosh Ghavami Riabi, Ameer Hamoodi, Shafee Rashidi, Zixian Chloe Wang, and Guy Nevo, who all played an essential role in the data collection process for Chapters 3 and 4 and helped me reach the end of this project.

Lastly, I want to express a special thank you to my sister and parents for their care and support throughout this process. Their encouragement and understanding were invaluable and I wouldn't be where I am without their love and guidance.

Contents

Lay Abstract **iii**

Abstract **iv**

Acknowledgements **v**

1 Introduction to Haptic Perception and Bayesian Analysis **1**

1.1 What is Perception? 1

1.2 Signal Detection Theory 2

1.2.1 Sensory Noise 2

1.2.2 The Two-Interval Forced Choice Task 4

1.3 Tactile Perception 5

1.4 Bayesian Inference 7

1.4.1 The Bayesian Brain 8

1.4.2 Cue Combination 9

1.5 Current Research Question 12

2 Mathematical Derivations & Computer Simulations **14**

2.1 A Quantitative View of The Two Interval Forced Choice Task . . . 15

2.2 Finding the Participant's Sensory Variance 20

2.3 Finding the Participant's Sensory Percept for the Three Finger Cue Conflict Condition 21

2.3.1 Cue Conflict Conditions 23

2.3.2 Calculations for Each Model 23

2.4 Model Comparison 24

2.5 Parameters of the Simulation 26

2.6 Simulation Results 27

2.6.1 Test-Retest Reliability Across Simulated Trials 34

3 Experimental Results **37**

3.1 Methods 37

3.1.1 Participants 37

3.1.2 Apparatus 37

3.1.3 Procedure 40

3.1.4 The Guessing Bayes Factor 41

3.2 Statistical Analysis 42

3.2.1 Results of Non-Conflict Cue Combination 43

3.2.2 Alternative Models 48

3.2.3 Model Comparison without Cue Conflict Data 50

3.2.4 Cue Conflict Data 51

3.2.5 Model Comparison With Cue Conflict Data 55

4 Technical Considerations and Pilot Study **57**

4.1 Questions About the Cue Conflict Condition 57

4.1.1 Cue Conflict Multi-Stimulus Piece 58

4.1.2 Home Position of the Cue Conflict Stimulus 60

4.1.3 Rotation of the Cue Conflict Edge 60

4.1.4 Speculative Analysis 61

4.2 Pilot Study 63

4.2.1 Methods of Pilot Study 63

4.2.2 Preliminary Results of Pilot Study 64

5 Discussion **69**

5.1 Sources of Error 72

5.1.1 Challenges in the Cue Conflict Paradigm 72

5.1.2 Infinite Sub-Optimal Models 72

5.1.3 Assumptions in our Analysis 73

5.1.4 Mechanical Considerations of Experiment 73

5.1.5 Effect of Covid-19 74

5.2 Future Directions 74

5.2.1 Pilot Study Insights 74

5.2.2 Manipulating Digit Acuity 75
5.2.3 Broader Applications 75
5.2.4 Conclusion 76

A Supplemental Derivations **77**

Bibliography **80**

List of Figures

2.1 Probability Density Functions 16
2.2 2IFC Task Description 17
2.3 Simulated Gaussian Difference Distribution 18
2.4 Psychometric Function, $\Psi(\Delta)$ 20
2.5 2IFC Task With a Cue Conflict 22
2.6 Simulated Psychometric Functions Under Models 28
2.7 Simulation Results of 70 Trials 30
2.8 Simulation Results of 140 Trials 31
2.9 Simulation Results of 300 Trials 32
2.10 Comparing σ_s of Two Simulated Blocks 36

3.1 Multi-Stimulus Cue Pieces 39
3.2 Support Pieces 40
3.3 σ_s on Day 1 vs 2 44
3.4 σ_s Posteriors for D2, D3, D4 and D234 45
3.5 Best Single Digit vs D234 σ_s 46
3.6 Observed vs Predicted D234 σ_s 47
3.7 D234 vs D2 σ_s 49
3.8 D234 vs D3 σ_s 49
3.9 D234 vs D4 σ_s 50
3.10 Model Posteriors, No CC Data 51
3.11 μ on Day 1 vs Day 2 52
3.12 CC μ Distribution 53
3.13 Model Posteriors, With CC Data 56

4.1 Original CC μ Distribution 58
4.2 Model Posteriors, Excluding +1.0 CC Condition 62

4.3 Pilot: Comparison of σ_s 64
4.4 Pilot: Comparing μ on Days 1 and 5 66
4.5 Pilot: Model Posteriors For Each Participant 67

List of Tables

2.1 D234 Percept and Sigma per Model 24
2.2 D234 PSE Shift per Model 24
2.3 Model Classification of Simulated Set 1, Without CC Data 33
2.4 Model Classification of Simulated Set 1, With CC Data 33
2.5 Model Classification of Simulated Set 2, Without CC Data 34
2.6 Model Classification of Simulated Set 2, With CC Data 34

3.1 The Average σ_s Value of Each Digit(s) 43
3.2 Categorization of Each Participant's Model, Excluding CC Data . . 51
3.3 The Average μ per CC Condition 54
3.4 Categorization of Each Participant's Model, Including CC Data . . 56

4.1 Categorization of Participants, Excluding CC Condition -1.0 mm from Data 62
4.2 Pilot: σ_s of Each Digit 65
4.3 Pilot: μ of Each CC Condition 65
4.4 Pilot: Categorization of Each Participant's Model, Excluding CC Data 68
4.5 Pilot: Categorization of Each Participant's Model, Including CC Data 68

List of Abbreviations and Symbols

Abbreviations

D — Data
H — Hypothesis
M — Model
2IFC — 2 Interval Forced Choice
OPT — Optimal (Bayesian)
AVG — Unweighted Average
WTA — Winner-Take-All
BAP — Bayesian Adaptive Procedure
MAP — *Maximum A Posteriori*
PSE — Point of Subjective Equality
PDF — Probability Density Function
CC — Cue Conflict
ITA — Index-Take-All
MTA — Middle-Take-All
RTA — Ring-Take-All

Symbols

$D2$	—	Digit 2 (i.e. the index finger)
$D3$	—	Digit 3 (i.e. the middle finger)
$D4$	—	Digit 4 (i.e. the ring finger)
$D234$	—	Digits 2, 3 and 4 together
Δ	—	The stimulus intensity of a given 2IFC trial
Ψ	—	The psychometric function
μ_2	—	Percept of D2
μ_3	—	Percept of D3
μ_4	—	Percept of D4
μ_{234}	—	Percept of D234
σ_2	—	Tactile acuity of D2
σ_3	—	Tactile acuity of D3
σ_4	—	Tactile acuity of D4
σ_{234}	—	Tactile acuity of D234
σ_s	—	Short for $\sigma_{sensory}$, the tactile acuity at 76% threshold of Ψ
μ	—	Perceptual bias/shift in Ψ

Declaration of Academic Achievement

I, Rose Jajarmi, declare that this thesis titled, **Investigation of Multi-Digit Tactile Integration: Evidence for Sub-Optimal Human Performance**, and works presented in it are my own. I confirm that for all chapters any work I completed was done by myself or with collaborative input from my research supervisor, Dr. Daniel Golreich, who in particular assisted in guiding data analysis and provided programming expertise. Any exceptions to this statement will be listed below.

- For Chapter 3 data collection was completed with the assistance of undergraduate students Kourosh Ghavami Riabi, Ameer Hamoodi, Shafee Rashidi, Zixian Chloe Wang, and Guy Nevo.
- For Chapter 4 pilot data was completed with the assistance of Kourosh Ghavami Riabi, Ameer Hamoodi, and Zixian Chloe Wang.

Chapter 1

Introduction to Haptic Perception and Bayesian Analysis

1.1 What is Perception?

In the realm of perceptual studies, the investigation of tactile perception boasts a rich and extensive history within both the fields of psychology and philosophy (Merleau-Ponty, 1962). This enduring pursuit of understanding how our physical surroundings shape our consciousness can be traced back to early Enlightenment thinkers like René Descartes, who grappled with these concerns while formulating the renowned "mind-body problem" (Ostenfeld, 2018). Descartes' distinction between the seemingly immaterial realm of the mind and the tangible substance of our physical bodies gave rise to the perplexing question of how these two domains could interact and exert influence on each other. This conundrum underscores the uncertainty surrounding the reliability of our senses in faithfully conveying the external world to our consciousness. Consequently, perception, defined as our conscious sensory experience, necessitated reevaluation and a more critical examination of its execution.

From a psychological standpoint, we can view conscious experience as an entirely physiological process. This perspective hinges on the assumption that even the ostensibly immaterial aspect of conscious perception is a product of intricate biological processes orchestrated by our nervous systems. Nevertheless, the ability

of biological organisms to utilize their neural circuitry for processing environmental cues is a complex and not easily elucidated endeavor. It is well-established that sensory stimuli elicit neural action potentials to encode information, and, in turn, our nervous system exhibits remarkable proficiency in decoding and interpreting the sensory information it receives to generate sensations from stimuli. Yet, comprehending this intricate and pivotal relationship between the external environment and internal perceptions requires detailed experimentation and observation.

In this context, the field of psychophysics assumes particular relevance, offering a vital tool for capturing the manifestations of these internal mechanisms and, in turn, shedding light on their operational principles.

1.2 Signal Detection Theory

Signal detection theory (SDT) marks an early attempt at formalizing our understanding of how perception functions (Green & Swets, 1996; Tanner Jr. & Swets, 1954). The advancement of SDT was a significant milestone in psychophysics (Treisman & Faulkner, 1985; Wixted, 2020), as it provides a structure by which analysis can be performed to test whether individuals are able to detect a signal irrespective of the presence of noise. Within this theory we find the explanation as to why an observer's decisions are fundamentally probabilistic. Thus, the stochastic character of an individual's perception, and their decisions made regarding it, is quantitatively accounted for as noise.

1.2.1 Sensory Noise

A crucial aspect of stimulus detection involves recognizing that the same stimulus presented to an observer can lead to varying internal perceptions. For instance, if we repeatedly expose an individual to an identical light stimulus, they may detect it in one trial but not in the next. This variability in both perception and response can primarily be attributed to the biophysical properties of the nervous system and the resulting noise it generates. It must be noted, however, that noise can be regarded as a pervasive element within the process of perception. For our

purposes, noise is defined as random or irregular fluctuations in neural activity not stemming from the source signal which significantly contributes to perceptual variability (Faisal et al., 2008). Biophysical properties, such as the initial state of an individual's neural circuitry, can thus be expected to undergo minute changes as a function of time before each trial in any perceptual task, even under controlled conditions. These changes can be considered to be one contributor to the general state of sensory noise present in the nervous system, though there exist other sources.

At the level of individual neurons, we observe membrane noise arising from the dynamics of ion channels. In neuronal networks, noise emerges from the convergence of numerous independent random synaptic inputs. Additionally, external factors introduced by the presentation of the stimulus to the observer add another layer of noise (Bialek & Setayeshgar, 2005). Even the noise present in how our motor systems move our body to interact with stimuli adds a level of complexity and noise to our nervous system (Frank et al., 2006). The multiplicity of noise sources underscores the intricate nature of perception and the challenges it poses in achieving consistent and precise stimulus detection.

The noise associated with a cue is often described as Gaussian when, through repeated sampling of that cue, the spread of the collected samples conforms to a normal distribution. This tendency for noise to exhibit Gaussian characteristics arises from the fact that noise can result from a variety of random events. These events encompass scenarios such as the dispersion of air molecules or the minute fluctuations in temperature, all of which can contribute to measurement imprecision and, consequently, introduce noise. This randomness is typically attributed to either thermodynamic or quantum mechanical factors. It should also be noted that this Gaussian distribution is found in the final stage of perception, and that at the level of neuronal firing the process is more apt to be described as a Poisson process due to the discrete stochastic firing rates present (Knill & Pouget, 2004; Tolhurst et al., 1983).

By employing central limit theorem we see that when sampling from distributions of the mean a large enough sample size will generate a normal distribution. Specific to our study purposes, this would refer to the process by which we take

multiple trials of a participant's responses on a perceptual task, thus sampling their internal measurement distribution. Consequently, being able to characterize this noise distribution quantitatively, through the measure of its mean (x) and variance (σ^2) is a valuable tool in assessing a feature of perception.

1.2.2 The Two-Interval Forced Choice Task

One method frequently employed to assess stimulus detection is the two-interval forced-choice (2IFC) task, wherein participants are tasked with choosing the correct option from two presented stimuli. For instance, in a typical 2IFC paradigm, a participant may sequentially hear two sounds and then be prompted to select which of the two they believe to be higher in pitch. This approach offers the advantage of allowing participants to weigh the sensations produced by the two stimuli relative to each other.

Furthermore, this method doesn't rely on the participant's subjective decision criteria, i.e. their personal assessment of the amount of stimulus required for them to acknowledge its presence. This is because the decision criteria is inherent in both presentations of the stimulus to the observer (Luce & Krumhansl, 1988).

When exploring signal detection theory, a natural point of interest arrives in the notion of a perception as a result of stimulus intensity (Green & Swets, 1996). Consequently, a mathematical function relating stimulus level and the probability of correct detection by an observer has been formalized and referred to as a psychometric function. Ψ. The psychometric function assumes that an observer has an internal probabilistic 'map' or rule which connects the stimulus intensity to the response, and that this map tends to be consistent within each observer. The psychometric function of a participant can only be determined through experimentation and the subsequent analysis of data the gathered. Usually a participant is tested and their response, either correct or incorrect, to varying intensities of a stimulus is recorded.

Originally, psychometric functions were perceived as step functions, implying a distinct boundary or threshold where stimuli transition from undetectable to

detectable. However, as our understanding evolved, we came to embrace a sigmoidal interpretation of these functions (Macmillan et al., 2022; Wickens, 2002). This change in perspective challenged the then conventional notion of a threshold as an absolute boundary. Instead, it portrays it as a point of transition within the sigmoidal curve. This nuanced perspective allows us to explore the intricate interplay between signal and noise in the perceptual landscape, ultimately refining our grasp of the threshold concept in signal detection theory.

However, the questions arises as to how one can succinctly compare psychometric functions between individuals, as such a comparison would lend itself well to data analysis. To this end, a threshold can be used for ease of analysis. In our research specifically, we use the participants' 76% threshold of their psychometric function as a point of reference, as it also serves as a measure of their sensory acuity (i.e. $\sigma_{sensory}$ or σ_s).

1.3 Tactile Perception

Within the expansive domain of perceptual studies, the investigation of tactile perception stands as a unique testament to the intricate relationship between our sensory experiences and the world around us. While much research has traditionally focused on our sense of vision and hearing, the significance of our sense of touch should not be underestimated, particularly in the context of navigating and comprehending our environment. Beyond merely allowing us to sense and perceive characteristics of stimuli, tactile perception, mediated by the intricate neural pathways of the somatosensory system, equips us with the remarkable ability to interact with our surroundings on an unparalleled level of precision and subtlety.

The human hand emerges as a central protagonist in this sensory narrative, representing itself as one of our most remarkable and versatile tactile organs. Its unique combination of sensitivity and dexterity facilitates interactions with our environment in ways that no other sensory modality can emulate. The sensory receptors, including mechanoreceptors embedded in the skin and distributed throughout the hand, play a pivotal role in detecting and transducing tactile information (Johansson & Flanagan, 2009). These specialized receptors respond to

mechanical stimuli such as pressure, vibration, and skin deformation, ultimately converting these physical cues into neural signals that are transmitted to the brain for processing (Handler & Ginty, 2021; Johnson, 2001).

Beyond immediate sensory-motor control, our hands act as exploratory instruments, enabling us to probe the intricate details of an object's surface. We can trace both the contours of familiar exteriors and navigate complex and unfamiliar terrains. In these moments, tactile perception not only informs us about the physical attributes of the objects we encounter but also enriches our emotional and cognitive experiences. In turn, this deepens our connection with our surroundings and in turn fosters a sense of presence and engagement.

The hand and its role in perception further exemplify the intricate relationship between our sensory experiences and the world. The brain's processing of cues from each digit of the hand highlights the remarkable sophistication of tactile perception. Each digit contributes unique sensory information, enabling us to differentiate between fine textures, temperatures, and shapes (Dargahi & Najarian, 2004). Notably, the hand is not just a tool for sensing but for grasping as well. The feedback which we receive guide our motor actions, ensuring the appropriate force is applied and that our grip adapts to the object's specific properties. And, as we interact with a stimulus, we also experience the shift in our sensory epithelium as the arrangement of our skin changes as we move (Handler & Ginty, 2021). The brain integrates this multi-dimensional input, allowing us to create a comprehensive and coherent perception of the objects we touch.

The brain has the remarkable ability to combine the data from each digit to create a holistic perception of an object's properties, seamlessly integrating information from multiple sources (Camponogara & Volcic, 2021). In our study we hope to capture this complex interplay by designing the experiment to allow for this active movement by participants, rather than relying on a participant's passive perception of the stimulus being applied to the hand.

However, it is worth noting that despite the hand's extraordinary capabilities and the richness of tactile perception, research in the field of touch has historically received less attention compared to vision. Even studies on tactile perception

seem to often employ the integration of visual and tactile cues in combination, rather than just focusing on the tactile modality (Camponogara & Volcic, 2021; Ernst & Banks, 2002; Riemer et al., 2019; Sathian et al., 2011). As a result, tactile perception, including the intricacies of hand perception, remains an area ready for exploration and discovery. Closing this gap in research can lead to a deeper understanding of the hand's role in perception and its broader implications for our cognitive and technological advancements. In addition to its immediate role in guiding motor actions and enriching our sensory experiences, the study of tactile perception in the hand holds broader implications for fields such as neuroscience, psychology, and technology. Understanding how the hand processes tactile information, how it differentiates between stimuli, and how it adapts to changing environmental conditions can shed light on fundamental questions about the organization of the brain, the nature of perception, and the development of innovative technologies, such as haptic interfaces and prosthetic limbs.

1.4 Bayesian Inference

Now that the discussion of how to measure the internal response of sensory data has occurred, we can further discuss possible models of how these cues combine to create a sensory percept. Before approaching this topic, let us begin with Bayes' Theorem (Bayes et al., 1763):

$$P(H_i|D) = \frac{P(D|H_i) \cdot P(H_i)}{\sum_{k=1}^{N} P(D|H_k) \cdot P(H_k)} \tag{1.1}$$

The benefit of Bayesian analysis is that it provides a posterior probability (denoted as $P(H_i|D)$) of one hypothesis, H_i, out of N total hypotheses occurring. It calculates this given the prior probability of a hypothesis (denoted as $P(H_i)$) as well as its likelihood (denoted as $P(D|H_i)$), where the likelihood is defined as the probability of the data, D, occurring under the assumption that the hypothesis is true. To illustrate with an example, if one is out on a walk late at night and perceived some sort of animal in the distance, we can create two hypotheses; hypothesis 1 is that the animal is a dog and hypothesis 2 is that the animal is a

coyote. Since you encounter more dogs in your neighbourhood, hypothesis 1 has a much higher prior, but given that you see the animal to be very large and walking menacingly the likelihood of the coyote hypothesis given this data is quite high. Thus, Bayesian analysis can mathematically weight the information appropriately to produce accurate predictions of which hypothesis is more probable, accounting for both what we have learned from the prevalence of scenarios (priors) and not disregarding current evidence (likelihoods). It also should be noted also that background knowledge impacts both our priors and likelihood.

Up to this point we've described Bayesian processing as a way to explain a perceptual process, but the same calculations can also be used for a statistical Bayesian analysis. The focus remains on modeling uncertainty using probability distributions and updating these distributions based on observed data. These methods allow one to make inferences about population parameters based on sample data. There are key differences found between the frequentest and Bayesian approach to statistics (Pek & Van Zandt, 2020). Rather than the common statistical tool of null hypothesis significance testing, Bayesian analysis formulates the posterior probability of each hypothesis (or model) to determine if the data favours one over the other. This is encapsulated within the a ratio of the marginal likelihoods of two hypotheses, formally referred to as the Bayes factor (Jeffreys, 1961). Bayesian statistics allows investigators to obtain a degree of belief in each of their hypotheses or models, which is in contrast to the frequentest approach of either rejecting or failing to reject the null hypothesis. As both methods have their respective advantages, in this thesis we will rely upon a combination of the two when approaching the data.

1.4.1 The Bayesian Brain

In the realm of human perception, a Bayesian framework, which employs the same principles applied in statistical analysis, offers a valuable perspective. It posits that the brain constructs a model of the external world, continuously adjusting it based on incoming sensory data (Rowe et al., 2020; Vetter & Newen, 2014). Even under this assumption, the task given to the nervous system to accomplish perception is no easy one; it must take in the neural impulses originating from our

sensory organs and decode the population response of neurons into some meaningful and coherent observation. This task seems even more challenging when considering, as previously mentioned, the variability inherent within perception. An identical stimulus typically does not consistently elicit the exact same neural response (i.e. action potential firing rate in each neuron). Furthermore, the brain must distinguish this specific neural response pattern from those generated by different stimuli. While some mystery remains, Bayesian inference provides a normative model against which to compare our processing of sensory information (Ghahramani, 1995; Rohe & Noppeney, 2015).

Accordingly, if we are to assume Bayesian reasoning is behind how the brain processes sensory information, then we are assuming that the brain perceives a stimulus characteristic H as a conditional probability $P(H|D)$ where D is the sensory data available to the brain. Generally, this would indicate that the brain is computing the likelihood of multiple possible values of the parameter H, and thereby allowing for optimal integration of additional information (Knill & Pouget, 2004).

We can then use this conceptualization to begin discussing more complicated experimental questions involving the integration of sensory cues within the brain and its relation to perception. For the purposes of this thesis, stimulus cues will specifically refer to the features of the stimulus presented to an observer, while a cue measurement will refer to the internal perception of the cue formed by an observer after presentation of the stimulus.

1.4.2 Cue Combination

The process of integrating multiple stimulus cues is a common aspect of our perceptual experience. However, comprehending how these cues come together to shape our perception poses a complex challenge, and can at times lead to surprising results.

For example, listening to another individual requires both an examination of the acoustics the speaker makes as well as the visual information conveyed by the configuration of the mouth and other facial features. This is demonstrated

by McGurk and MacDonald (1976) in the *McGurk effect*, in which a participant was exposed to a film of a woman speaking [ba] but had been dubbed onto lip movements for [ga] and as a result adult participants heard [da]. This striking example highlights how an auditory cue can be significantly influenced by the presence of another cue, in this case, a visual one.

Another classic example of multi-sensory processing and cue combination is the *ventroliquism effect*, in which observers, when simultaneously presented with an auditory and visual stimulus, will report that the auditory source is closer to the visual source than it truly is (Bruns, 2019). A study by Alais and Burr (2004) has shown that this effect was regulated by the respective reliability of our visual and auditory cues, indicating that perception was influenced by the more reliable cue, which is typically visual.

The *rubber hand illusion* is another phenomenon that arises from tactile and visual cue combination, to create a coherent perception of one's body (Riemer et al., 2019). To produce this illusion, a participant's real hand is hidden from view, and a lifelike rubber hand is placed in a similar position. When both the real hand and the rubber hand are synchronously stroked, most participants begin to feel as though the rubber hand is their own. They report a sense of ownership and body awareness toward the rubber hand, even though they logically know it's not their real hand.

To better understand the interplay between multi-modal cue integration, we can look to Bayesian models once more. Bayesian models serve as normative frameworks in the field of perception and decision-making, providing optimal strategies for processing sensory information and making inferences. While these models represent the idealized approach, human cognition often operates within the realm of bounded rationality. While humans are not expected to be perfectly Bayesian, as that would require a level of computational perfection that is rarely attainable, research in cognitive psychology and neuroscience has shown that humans can often approximate Bayesian principles in their sensory perception and decision-making processes (Ernst & Banks, 2002; Knill & Pouget, 2004; Rohe & Noppeney, 2015). We may not reach the pinnacle of Bayesian optimality, but we tend to approach it to varying degrees. However, the question arises as to what would it appear as

for a human observer to be either Bayes' optimal or not, which is one we will now explore.

1.4.2.1 Winner-Take-All Model

Let's begin by exploring what would happen if the brain didn't integrate cues from stimuli sources. One alternative approach could be the 'winner-take-all' (WTA) model, which involves focusing solely on the cue provided by the sensory system with the least noise (i.e. greatest acuity), indicated by the smallest σ when modeled as a Gaussian distribution. While this strategy may appear plausible and resource-efficient, it can fall short in terms of accuracy and efficiency compared to a model that fully embraces the integration of multiple cues. Relying on only one cue, even if the sensory system processing it is the most reliable, means that the resulting sensory percept is still subject to the noise inherent within the sensory processing system. Even adding less reliable sensory cues can sharpen our ability to pinpoint the characteristics of stimuli detected accurately. In order for the brain to accomplish this, then, it must know at minimum which sensory cue has the best acuity in order to disregard other cues it is given.

1.4.2.2 Unweighted Average Model

Another possible model the brain could use to combine cues is the unweighted average model (AVG). Under the average model, cue combination is achieved by taking the mean of all cues to form a percept of a stimulus. As a result, each cue can influence an observer's final percept equally. While the potential advantage of this model is that the observer is considering more information, the drawback is that this model is more vulnerable to error caused by cues that have low reliability. In other words, if all cues are rated equal, even cues from a sensory modality that is less accurate, an observer's perception will likely be skewed towards the more inaccurate stimuli. Alternatively, the benefit of this approach could lie in the fact that the brain does not need to 'contrast' the acuity of the cues it receives, it only needs to average them.

1.4.2.3 Optimal Model

Finally, we can consider the optimal (OPT), i.e. Bayesian, method of cue combination. While discussing the previous possible models, it becomes apparent that an optimal model should both include all possible cues *and* appropriately weight each cue according to its accuracy. In the case that the reliability of different cues changes as a result of experimental parameters, an optimal Bayesian observer would weight cues on different trials accordingly. Similar to the WTA model, the brain in the OPT model is assumed to know the acuity of each of the cues it receives, in order to produce this percept. Assuming each cue is processed independently of the other and that a Gaussian function can model the distribution of each measurement, we will have the following equation for an observer's mean percept where w_i and μ_i are the i^{th}'s cue's respective weight and value.

$$\mu_{sensory} = w_1\mu_1 + w_2\mu_2 + w_3\mu_3 \tag{1.2}$$

The weight of each cue can be derived from Bayes formula through the product of the likelihoods such that $w_i = \frac{\frac{i}{\sigma_i^2}}{\sum_k \frac{1}{\sigma_k^2}}$.

1.5 Current Research Question

Considering the intricate nature of the somatosensory system, our objective was to investigate whether the brain optimally combines tactile cues. To our knowledge, there has been limited prior research on the integration of tactile-tactile cues, and thus, this study seeks to fill this gap in the existing literature. To achieve this, we will concentrate on a stimulus edge presented to the index, middle, and ring fingers, assessing the acuity of each digit individually. Furthermore, we will evaluate participants' tactile acuity when the stimulus is simultaneously applied to all three digits to determine how the sensory perception of the cue was integrated by the participant. Additionally, the integration of these cues will be assessed following the application of a cue conflict paradigm. In this paradigm, the edge stimulus presented to all three digits simultaneously is modified from its usual straight-edge

form, resulting in a slight positional discrepancy for each digit. Previous research in this lab by Prodribaba (2018) suggested that optimal cue combination of tactile cues was not achieved by participants. However, we have improved upon the initial study design by increasing the participant's hand stability and by introducing an informative cue conflict paradigm, in the goal of determining the validity of these results with further testing. The results of our experiment will allow us to better determine which possible model of cue integration the participant employs, and thus better our understanding on the strategies the brain employs when combining tactile cues in complex sensory environments.

Chapter 2

Mathematical Derivations & Computer Simulations

While our primary objective is to investigate human tactile perception, it is essential to comprehend how such data will be categorized within our analyses. Given this, we can simulate human participant responses using computer programs. The advantage of this approach is twofold: it serves as a reflection of what we might expect in the actual experiment and as a proof of concept. By simulating the data and subsequently conducting Bayesian data analysis, we can evaluate the effectiveness and accuracy of our methods. However, to create any such simulation, we must first outline the procedure for our experiment.

The actual experiment will span two days, with both days involving the participant undergoing 8 blocks, each consisting of 70 trials of the 2IFC task. The first 4 blocks will exclusively test either the index (D2), middle (D3), ring finger (D4), or all three digits simultaneously (D234; see Figure 2.2a for a visual of how the 2IFC is performed on D234). The remaining 4 blocks will assess all three fingers

simultaneously but will each include a cue conflict (CC) of either $+1.0$, $+0.5$, -0.5, or -1.0 mm.

In order to simulate experimental data, we programmed a computer to select the sensory acuity of a participant's individual digits by sampling from specified normal distributions. Each simulated participant was additionally assigned a cue combination strategy as the method (i.e. model) employed by each participants. Then simulated was their responses for each 2IFC trial, indicating whether they correctly or incorrectly discriminated the stimulus on each trial. Subsequently, we can analyze these results and compute the probability of each model being used.

To understand how the program will function, we must first introduce the quantifiable aspects of the 2IFC task and the subsequent data analyses which will be performed.

2.1 A Quantitative View of The Two Interval Forced Choice Task

Referring to a previously mentioned point of the uncertainty due to internal noise, it is important to note that the internal representation of the stimulus is generally conceptualized as the result of a normal probability distribution function (PDF). This PDF has a horizontal axis representing the internal response and a vertical axis representing the probability of that internal response occurring given the stimulus. If we take the two stimuli in the 2IFC, each produce a PDF of some internal response within the participant's neural circuitry, as in Figure 2.1 (Heeger, 1997).

When delving into psychophysical processes, the 2IFC task, or its variants, frequently emerges. A 2IFC task relies upon the participant being presented with two observation intervals in succession and then being asked to draw comparisons in their perception. In our experimental design, we ask the participant to discriminate between the relative positions of an edge which the digit(s) of the hand tap down on twice sequentially. The edges' positions will be separated by a distance of Δ in each case (see Figure 2.2b). Regardless of the order in which the tap

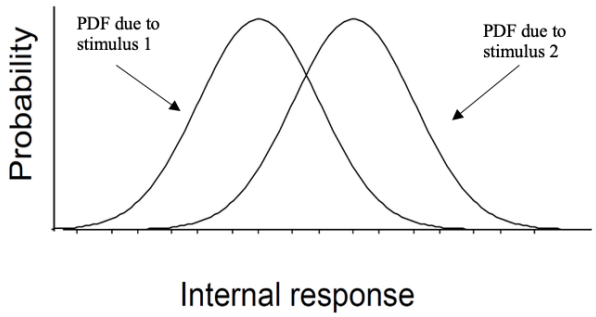

Figure 2.1: Probability Density Functions. Depiction of the probability density functions arising from two stimulus cues. The probability of a certain level of internal response occurring is shown as the height of the curve.

is applied, we can characterize the two edges by their relative position, referring to the distal edge measurement (i.e. the edge closer to the tips of the fingers) as X_D and the proximal edge measurement (i.e. the edge closer to the palm) as X_P. Consequently the question at hand becomes what is the probability that X_D will be correctly characterized as the distal edge for each separation of Δ given? Note that since during the actual task the participant will be asked to determine whether the second edge they contacted was more proximal or distal relative to the first, we see that in doing so they must have first reflected upon the positions of each edge. Thus our reframing of the problem holds.

We can further restate the above question, in this task we are essentially looking to find the psychometric function of the participant. The psychometric function is one which describes the relationship between a stimulus level (the independent variable) and the probability of a behavioural response (the dependent variable) occurring. While there are several methods of obtaining the psychometric function, the one we are interested in arises from the results of the 2IFC task, as will be soon outlined (Klein, 2001).

We can begin by assuming that each edge percept results from the brain selecting a position for that edge, x_P and x_D, from some internal measurement of each stimulus represented by a Gaussian distribution (see Figure 2.1 B). This Gaussian distribution will be centred at the true position at which the distal or proximal

edge contacted the digit (x'_D or x'_P), and will have a standard deviation of σ_s related to the participant's acuity (here s is short for sensory, as this is the σ value associated with the participant's sensory perception). Accordingly, individuals with high acuity in their digits will have a smaller σ_s.

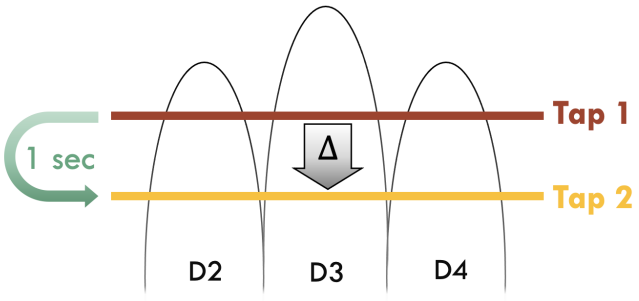

(a) A sample of how the 2IFC task would perform on the index (D2), middle (D3) and ring fingers (D4).

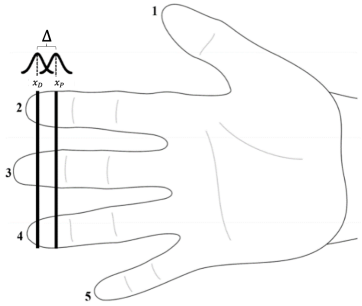

(b) A depiction of the internal measurement of where the proximal and distal edge are located are both drawn from a Gaussian centred at the true location of each edge

Figure 2.2: 2IFC Task Description. A visual illustration of the 2IFC task and the distribution of taps applied to the hand's digits.

If x_D and x_P represent the participant's percept of where the distal edge and proximal edge are, respectively, then we are looking for instances where $x_D - x_P > 0$, as such cases indicate that the participant is correctly identifying the positions of the two edges. Expanding this further, we can create a new Gaussian constructed by taking the distribution of the difference scores between the two initial Gaussian distributions representing the internal measurements of the distal and proximal edges (see Figure 2.2).

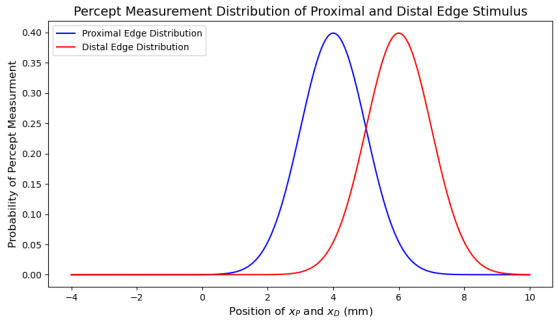

(a)

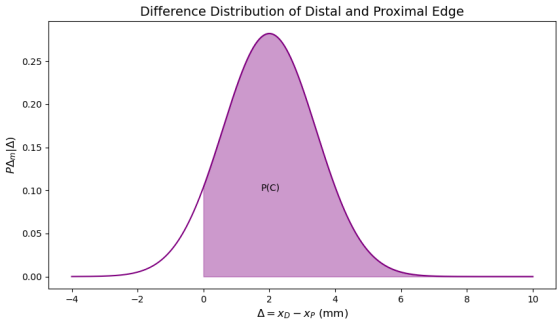

(b)

Figure 2.3: Simulated Gaussian Difference Distribution. (a) the probability of a participant's internal measurement occurring after tapping down on the proximal edge where $x'_P = 4$ mm and the probability of their internal measurement occurring after tapping down on the distal edge where $x'_D = 6$ mm. In both graphs the participant has a standard deviation of $\sigma_s = 1$. (b) the difference Gaussian is depicted with a mean of $\Delta = 2$ and a standard deviation of $\sigma = \sqrt{2}$.

This difference Gaussian will have a mean of $\Delta = x'_D - x'_P$ and a standard deviation of $\sigma = \sqrt{\sigma_s^2 + \sigma_s^2} = \sqrt{2} \cdot \sigma_s$. We further see how the participant draws from this difference Gaussian such that their probability of drawing a measurement $\Delta_m = x_D - x_P$ is shown in Equation 2.1.

$$P(\Delta_m|\Delta) = \frac{1}{\sigma\sqrt{2\pi}} \exp - \frac{(\Delta_m - \Delta)^2}{2\sigma^2} \tag{2.1}$$

Our next step is determining how to translate this probability into a psychometric function, which will model a participant's rate of correctly detecting the

stimulus of our 2IFC task. To start, it is clear that for any Δ_m drawn from this difference Gaussian the participant will only answer correctly when $\Delta_m > 0$. Thus, if we were to integrate the area under the curve from $\Delta_m = 0$ to $\Delta_m = \infty$ we would have the probability of the participant responding that the comparison is more distal for this trial (Equation 2.2).

$$P(\text{`Comparison Distal'}|\Delta) = \int_0^\infty \frac{1}{\sigma\sqrt{2\pi}} \exp -\frac{(\Delta_m - \Delta)^2}{2\sigma^2}\, d\Delta_m \tag{2.2}$$

Now that we have our integral, we can perform a series of operations to manipulate it into a form that is more suited to our purpose. We can first shift the Gaussian to center on 0 and shift the bounds of the integral accordingly.

$$P(\text{`Comparison Distal'}|\Delta) = \int_{-\Delta}^\infty \frac{1}{\sigma\sqrt{2\pi}} \exp -\frac{(\Delta_m)^2}{2\sigma^2}\, d\Delta_m \tag{2.3}$$

Next, since our Gaussian distribution is now symmetric and centered on 0 we realize that the integral from $-\Delta$ to ∞ equals the integral from $-\infty$ to Δ.

$$P(\text{`Comparison Distal'}|\Delta) = \int_{-\infty}^\Delta \frac{1}{\sigma\sqrt{2\pi}} \exp -\frac{(\Delta_m)^2}{2\sigma^2}\, d\Delta_m \tag{2.4}$$

Finally, we see that the probability of a participant responding correctly to the 2IFC task is simply the value of the cumulative normal distribution of our difference Gaussian, with a mean of 0 and a standard deviation of $\sqrt{2} \cdot \sigma_s$, at Δ. The psychometric function of the participant can be determined, and will appear as shown in Figure 2.4.

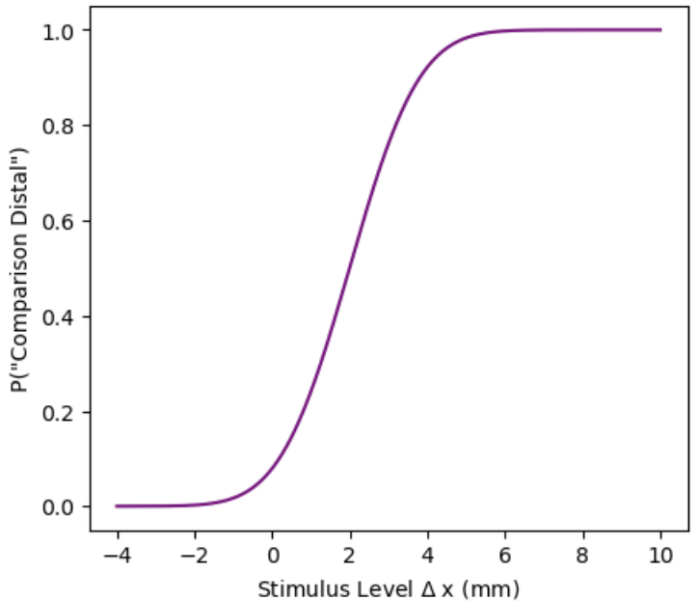

Figure 2.4: Sample Psychometric Function, $\Psi(\Delta)$. The resulting psychometric function from the Gaussian distribution of differences, relating the probability of a participant correctly comparing the location of the two stimuli relative to each other.

2.2 Finding the Participant's Sensory Variance

We will now examine how we may find the posterior probability of each digit's σ_s given a participant's performance on the 2IFC task. First, we will consider that each digit has a σ_s that is some value between 0.1mm to 7.00mm, as we are confident the true value of σ_s exists within this range. We can capture this range by taking a series of intervals that cover it. Such intervals, in mm, would appear as $[0.05, 0.15), [0.15, 0.25), ..., [6.95, 7.05]$. Consequently, the hypotheses for each σ_s is taken as the midpoints of each of these intervals (i.e. $H_1 = 0.1$, $H_2 = 0.2, ...$, $H_{700} = 7.0$). We apply a uniform prior probability to these hypotheses.

Our next step involves determining the posterior probability for each possible hypothesis, which can be determined quite straightforwardly by using a likelihood function to evaluate the data, D, as will be shown in the steps below.

In the previous section we laid the foundation of how we may determine the probability of a participant getting a correct response in a specific trial with edge separation Δ and their given σ_s. We can represent this probability as $\Psi(\Delta)$, and consequently the probability of the participant being incorrect is $1 - \Psi(\Delta)$. It follows then that for each hypothesised σ_s we can multiply the probabilities of the participant responding as they did, either correctly or incorrectly, for each trial separation and combine that all together.

$$P(d_k|\sigma_s) = \Psi(\Delta_k)^{c_k} \cdot (1 - \Psi(\Delta_k))^{i_k} \tag{2.5}$$

$$P(D|\sigma_s) = \prod_{k=1}^{N} P(d_k|\sigma_s) \tag{2.6}$$

Note that d_k represents the data obtained for a specific separation of Δ in the form of c_k and i_k, which are, respectively, the number of times the participant correctly and incorrectly responded to that separation of Δ in the 2IFC task. N represents the total number of Δ values which took place in the participant's block.

Ultimately, if we apply this method to each hypothesized σ_s we will have produced the likelihood of each σ_s for each digit(s) tested. To then form the posterior PDF, Bayes Theorem is applied (see Equation 1.1) using the respective likelihood value and prior probability of each hypothesis. Since we are assuming a uniform prior, $P(\sigma_s)$, the term cancels out and all that remains is the final posterior PDF $P(\sigma_s|D) = \frac{P(D|\sigma_s)}{\sum_k P(D|\sigma_{s_k})}$. From this posterior we can extract the *maximum a posteriori* (MAP) probability estimate, i.e. the mode of the posterior.

2.3 Finding the Participant's Sensory Percept for the Three Finger Cue Conflict Condition

In the previous sections, we assumed that the placement of a single tap was constant across all three fingers. However, this will no longer be the case during the

cue conflict task, as the first tap will apply an edge stimulus with different positional cues and thus require modifications to the previously outlined procedure (see Figure 2.5). Given that each digit will receive a different presentation location of the stimulus, then we can label the resulting perceptual bias in the percept location (i.e. a shift in the PSE) as μ.

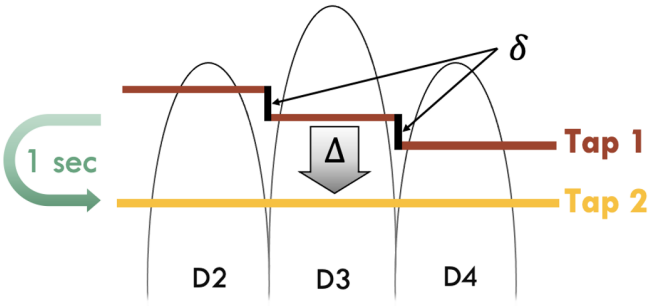

Figure 2.5: 2IFC Task With a Cue Conflict. In this version of the 2IFC task, the first presentation of the reference stimulus (tap 1) provides a conflicting cue presentation by a value of δ to the participant in comparison to the second presentation of the non-conflict comparison stimulus (tap 2).

Like before, we will create a range of hypotheses indicating possible σ_{234} and μ values. Likewise, hypotheses for σ_{234} consist of the midpoints of each interval ranging from 0 mm and 7.01 mm (i.e. $H_{\sigma 1} = 0.1$, $H_{\sigma 2} = 0.2, ...,$ $H_{\sigma 700} = 7.0$). For μ the hypotheses consisted of 161 values in steps of 0.05, beginning at -4.00 mm and ending at 4.00 mm (i.e. $H_{\mu 1} = -4.00$, $H_{\mu 2} = -3.95, ...,$ $H_{\mu 161} = 4.00$). We can then, for each hypothesized σ_s, evaluate which μ would have the highest probability given the participant's responses. Note that the value of $\Psi(\Delta)$ would be calculated similarly, with the exception that the psychometric function Gaussian used would no longer have a mean equal to 0, but to the value of any potential H_μ.

$$P(d_k|\mu, \sigma_{234}) = \Psi(\Delta_k)^{c_k} \cdot (1 - \Psi(\Delta_k))^{i_k} \tag{2.7}$$

$$P(D|\mu, \sigma_{234}) = \prod_{k=1}^{N} P(d_k|\mu, \sigma_{234}) \tag{2.8}$$

The result of these calculations would be a joint likelihood function, in which the probability of the data is dependent upon both a hypothesized σ_{234} and μ. For our purposes, we can treat σ_{234} as a nuisance variable and focus our attention on μ by marginalizing over σ_{234}. This results in us taking the summation for all probabilities with the same σ_{234} hypothesized, leaving only a distribution of probabilities dependent on μ. Like earlier, we can calculate the posterior probability by implementing Bayes formula (Equation 1.1) with the above likelihood and assuming a uniform prior.

$$P(\mu|D) = \sum_{\sigma_{234}} P(\mu, \sigma_{234}|D) \tag{2.9}$$

2.3.1 Cue Conflict Conditions

While the above descriptions of cue combination are relatively straightforward, what is less apparent is how tactile cues are combined when the cues themselves are conflicting from what the observer believes to be occurring.

2.3.2 Calculations for Each Model

Each model will have different associated ways of calculating the resulting psychometric functions that occur when tactile cue integration occurs. The ways in which σ_{234} and μ are calculated are listed in Table 2.1. See Appendix A for derivation of σ_{234} under the OPT and AVG model. The perceptual bias for each model predicted during the CC conditions is also shown in Table 2.2. See Appendix A also for the derivation of the perceptual bias under the OPT model.

Table 2.1
D234 Percept and Sigma per Model

Model	Percept (μ_{234})	Sigma (σ_{234})
OPT	$\mu_{234} = \frac{\frac{x_2}{\sigma_2^2}+\frac{x_3}{\sigma_3^2}+\frac{x_4}{\sigma_4^2}}{\frac{1}{\sigma_2^2}+\frac{1}{\sigma_3^2}+\frac{1}{\sigma_4^2}}$	$\sigma_{234} = \sqrt{\frac{1}{\frac{1}{\sigma_2^2}+\frac{1}{\sigma_3^2}+\frac{1}{\sigma_4^2}}}$
AVG	$\mu_{234} = \frac{x_2+x_3+x_4}{3}$	$\sigma_{234} = \frac{\sqrt{\sigma_2^2+\sigma_3^2+\sigma_4^2}}{3}$
WTA	$\mu_{234} = x_{\sigma_{min}}$	$\sigma_{234} = \sigma_{min}$

Table 2.2
D234 PSE Shift per Model.

Model	PSE shift (μ)
OPT	$\left(\frac{\frac{1}{\sigma_2^2}-\frac{1}{\sigma_4^2}}{\frac{1}{\sigma_2^2}+\frac{1}{\sigma_3^2}+\frac{1}{\sigma_4^2}}\right)\delta$
AVG	0
WTA	$-\delta, 0$ or $+\delta$

δ = -1.0, -0.5, +0.5 or +1.0 mm, and is determined by the CC condition.

2.4 Model Comparison

We have now established our three primary models and ascertained a method to calculate the posterior probability of a participant's σ_s and μ for each finger and all three fingers combined. The next question is determining which model is the most likely given a participant's data. Looking back to Bayesian analysis, when we have an exhaustive set of N models (i.e. $M_1, M_2, ..., M_N$) we can reformulate

Bayes' formula in the following way.

$$P(M_i|D) = \frac{P(D|M_i)P(M_i)}{P(D|M_1)P(M_1) + ... + P(D|M_N)P(M_N)} \tag{2.10}$$

An important caveat here, however, is that in order for the above expression to remain reasonable, each possible model should be included within our list of N models. And while there is just one optimal model, there are nearly infinite sub-optimal models that could be employed by an observer. Thus for the purpose of our analyses, we will assume that the priors for models not included in our analyses are close to 0, and thus the expression is still valid. For the purposes of our study we will also assume there is an equal prior probability for all the models we consider.

To calculate the likelihood of a given model M we can use the marginal likelihood formula.

$$P(D|M) = \sum_i P(D|\mu, \sigma_{234})P(\mu, \sigma_{234}|M) \tag{2.11}$$

The data consists of the responses across trials in blocks across the four CC conditions, which we will denote as D_{cc1}, D_{cc2}, D_{cc3} and D_{cc4}, as well as the non-conflict three finger condition, D_{cc0}. To find $P(D|\sigma_{234}, \mu)$ we will need to take the product of all probabilities calculated by each condition in the data, as shown in Equation 2.12. .

$$P(D|\mu, \sigma_{234}) = \prod_{k=0}^{4} P(D_{cc_k}|\mu, \sigma_{234}) \tag{2.12}$$

To find $P(D|M)$, we should first turn our attention to finding the value of $P(\sigma_{234}, \mu|M)$. Computationally, for a single participant, this is done by running 5000 trials, where in each we sample a value of σ from the known posterior of each digit (i.e. getting a sample of σ_2, σ_3 and σ_4). This sample is proportional to the values of the posterior it is drawn from, ensuring that most samples are appropriately centred on the mode of the posterior. While this is a relatively straightforward process, the more challenging task is to determine μ, which will shift in each trial of the 2IFC task according to Δ. If we recall from Table 2.1, we

can find the value of our percept under each model. For example, in the optimal model $\mu = \frac{\frac{x_2}{\sigma_2^2}+\frac{x_3}{\sigma_3^2}+\frac{x_4}{\sigma_4^2}}{\frac{1}{\sigma_2^2}+\frac{1}{\sigma_3^2}+\frac{1}{\sigma_4^2}}$ which can be further simplified to $\mu = \Delta + \left(\frac{\frac{1}{\sigma_2^2}-\frac{1}{\sigma_4^2}}{\frac{1}{\sigma_2^2}+\frac{1}{\sigma_3^2}+\frac{1}{\sigma_4^2}}\right)\delta$. Thus, as we know both the trial's condition (δ) and the tap separation between the reference and comparison cues (Δ), we can determine our value of μ. After 5000 trials in which σ_{234} and μ are calculated (and dividing these distributions by the number of trials) we will have formed a natural likelihood distribution of both results. In other words, σ_{234} and μ will be appear in the computer program at a rate related to their likelihood.

To determine $P(D_{cc_k}|\sigma_{234}, \mu)$ for $k = 1, 2, 3\, and\, 4$ we need only to follow the steps in Section 2.3, specifically Equations 2.7 and 2.8, for each trial where we sample our σ_{234} and μ), take the sum of all these values (and as stated above, divide by the number of trials run), and finally we will have found $P(D|M)$.

Now that all the missing pieces are present, it will be possible to calculate $P(M_i|D)$ in Equation 2.10 and we can obtain the probability model of each model being the one applied.

2.5 Parameters of the Simulation

While we have touched upon cue combination models in Chapter 1, we will now begin to apply how such models can be used by a computer program, to mirror human participants.

Before starting the simulation we must choose what the σ_s of our 24 participants will be for each of their digits. For demonstrative purposes I have chosen two sets of distributions from which σ_s will be drawn from. For the first set of simulations (Set 1) each of the 24 participants will have a σ_s drawn from Gaussian distributions of the index, middle and ring digits with means of 1.0 mm, 2.0 mm, and 4.0 mm respectively. The second set of distributions (Set 2) will similarly be drawn from Gaussian distributions of the index, middle and ring digits with means 2.0 mm, 2.2 mm and 2.5 mm respectively. In all of these Gaussian distributions the variance was 0.3.

The purpose in running the simulation twice, with two separate sets of σ_s, is to demonstrate how varying the σ_s may impact the ability of the analyses to distinguish which model is being employed. For example, in Set 1 where the σ_s are quite different from each other, it may be quite apparent when the AVG model is used, but less clear whether the OPT or WTA model is used. In Set 2 of the σ_s where they are all similar values to each other the issue is now the inverse; it is now difficult to distinguish between a optimal model and the average model, but easier to see if the winner-take-all model is being used. When the experiment is conducted on human participants we expect to see a range of σ_s combinations for the digits each participant, thus it is beneficial to highlight how any such distribution may be biased.

Now that the σ_s of each participant has been chosen, the simulation proceeds by simulating the performance of the each participant on the 2IFC task. On this we will also vary the number of trials present to demonstrate how increasing the number of trials per block. Thus, we will run the simulation three times per set of σ_s varying the number of trials from 70, 140 and 300 per block effects the analyses. The expectation with this variation is that with increased trial length comes increased accuracy in our analyses.

With our simulation we can also predict the shape of the psychometric function of the under each model as shown in Figure 2.6. Under the WTA model (2.6a, we expect the psychometric function of the best finger to match the three-finger psychometric function. Conversely, we see that the psychometric function in the three finger condition to be an average of three single digit psychometric function under the AVG model, and that the psychometric function in the three finger condition is expected to be better than all three digits alone in the optimal model.

2.6 Simulation Results

From using model comparison on the simulated 2IFC data, we can now determine $P(M|D)$ for each of our stated models. Thus we can form a distribution of these probabilities as shown in Figures 2.7 - 2.9b. Analyses were conducted on both Set

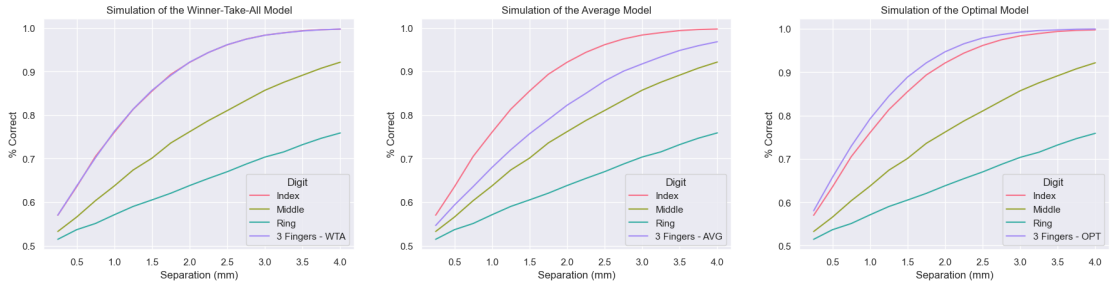

(a) WTA $\Psi(\Delta)$ **(b)** AVG $\Psi(\Delta)$ **(c)** OPT $\Psi(\Delta)$

Figure 2.6: Simulated Psychometric Functions Under Models. The depiction of the psychometric function given σ_s Set 1 ($\sigma_2 = 1.0$ mm, $\sigma_3 = 2.0$ mm, $\sigma_4 = 4.0$ mm under each model of cue combination. Note that under the WTA model (a) the best finger's psf (i.e. the index finger) overlaps with the three finger psf.

1 and 2 and over each tested block trial length (70, 140 and 300) and performed twice, once without the data on the cue conflict blocks and once with.

On σ_s Set 1 (see Figures 2.7a 2.8a 2.9a) we see a clear trend for the cases where the OPT model is the one being employed to combine cues, in which it the model comparison analysis classifies the OPT model, WTA model and AVG as the most likely models respectively. In the case where the AVG model is the one used, we observe that the AVG, WTA, and then OPT models are the most likely respectively. Finally, when the WTA model is the one used, the WTA, OPT and then AVG models are the most likely respectively.

Note that in the case where only 70 2IFC trials are simulated and cue conflict data is not included is when the analysis is most prone to wrongly classify the data. More specifically, under Set 1 it is most difficult to distinguish between the OPT and WTA models when one is employed under these conditions. This is because the in Set 1 the average of σ_s is ≈ 1.53 mm, which is quite distinct from the optimal σ_s (≈ 0.94 mm) and winner-take-all σ_s (≈ 1.00 mm). But, as we can see, the optimal and winner-take-all σ_s are much closer to each other, leading to the resulting difficulty in distinguishing the two without sufficient data.

Conversely, let's observe the results of the simulation for Set 2 (see Figures 2.7b 2.8b 2.9b). In the figures where the OPT model is used the most likely classifications are the OPT, AVG and then WTA model respectively. When the

AVG model is used to combine cues the OPT, AVG and then WTA are the most likely respectively when analysing without cue conflict data, and the trend becomes AVG, OPT and WTA when using cue conflict data. Finally, when the WTA model is used, the highest distributions of probability are WTA, AVG and then OPT respectively.

If we do the same as we did for Set 1 and calculate the approximate values for σ_s under each model for Set 2, then we can better make sense of why the analysis would classify the data as it did. Here we see that the optimal σ_s is ≈ 1.32 mm, the average σ_s is ≈ 1.29 mm and the winner-take-all σ_s is ≈ 2.00 mm, which explains why the OPT and WTA models were more likely to be wrongly classifed as the other in the analysis.

For each of these simulations, when the number of simulated 2IFC trials run is increased from 70 to 300 and the cue conflict data is included, the distribution trends described becomes further exaggerated and more accurate in their classification.

In addition to finding the distribution of the posterior probabilities of each model for each condition listed, the winning model (i.e. the model with the largest posterior probability of the three for each participant) has been tabulated.

In Tables 2.3 and 2.4 we can have the resulting classifications for each participant with our without the cue conflict data present in the participants simulated under Set 1. Again, we see that the accuracy of our analysis improves with the cue conflict and with more trials, with the most easily distinguishable model as the AVG model. In Tables 2.5 and 2.6 we again show the final classifications for participants under Set 2, with the WTA being the most easily distinguished model.

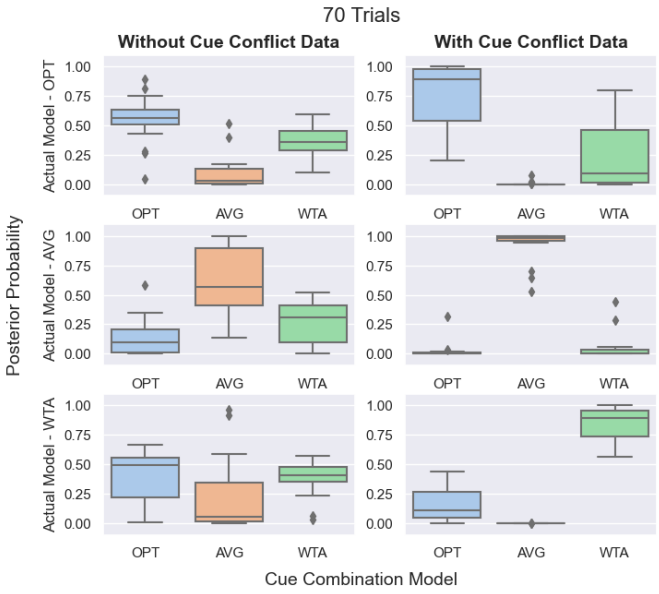

(a) Model Posteriors For Set 1 σ_s.

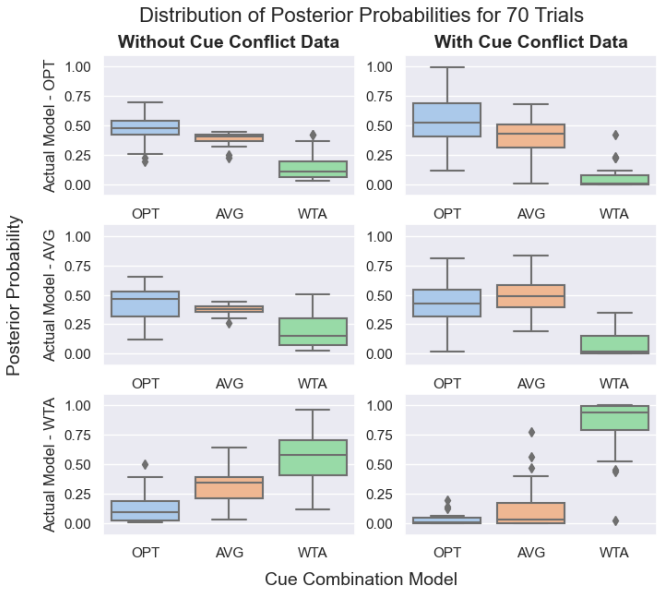

(b) Model Posteriors For Set 2 σ_s.

Figure 2.7: Simulation Results of 70 Trials. 70 2IFC responses were simulated, and the resulting probability of each model for all participants are shown in the boxplot for each distribution set. Also shown are the probabilities with and without the cue conflict data for comparison.

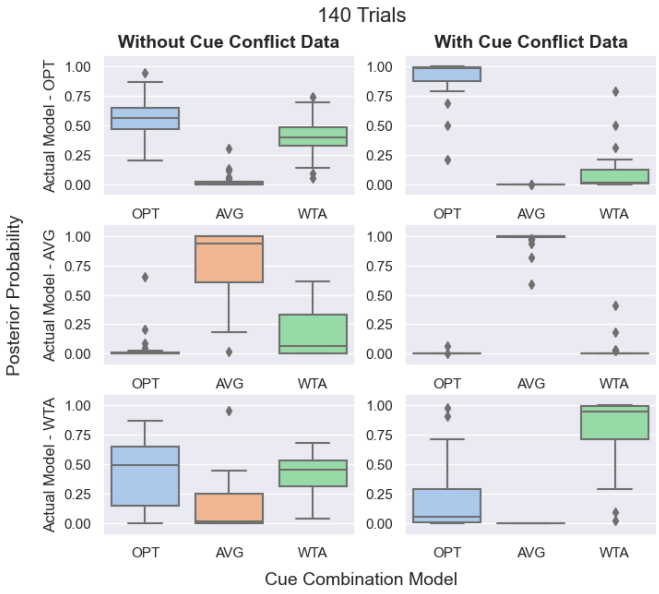

(a) Model Posteriors For Set 1 σ_s.

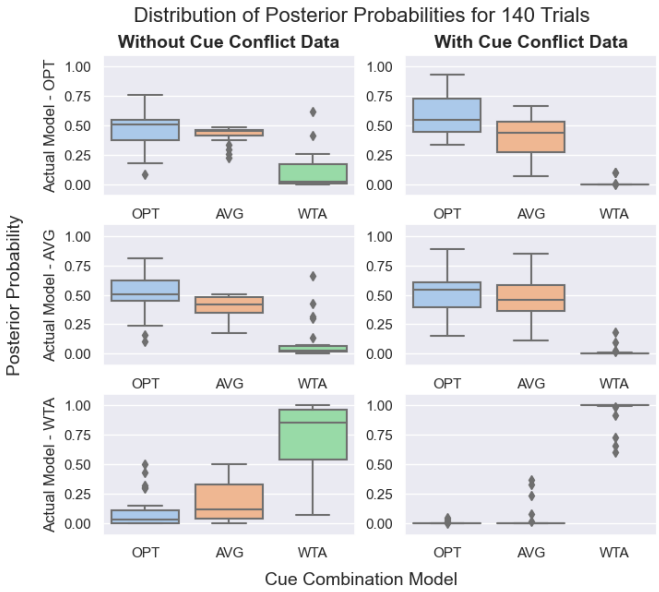

(b) Model Posteriors For Set 2 σ_s.

Figure 2.8: Simulation Results of 140 Trials. 140 2IFC responses were simulated, and the resulting probability of each model for all participants are shown in the boxplot. Also shown are the probabilities with and without the cue conflict data for comparison.

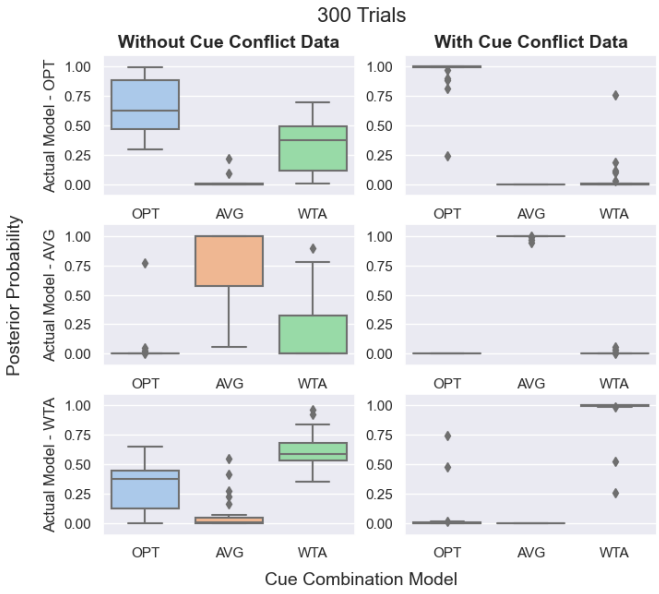

(a) Model Posteriors For Set 1 σ_s.

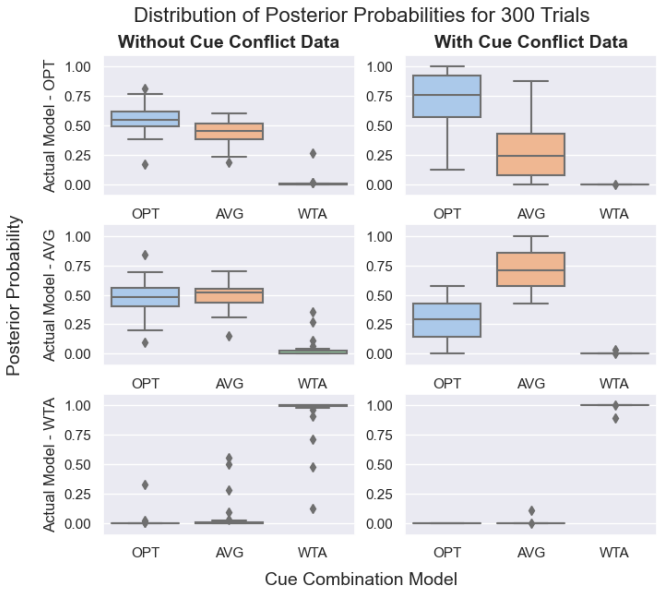

(b) Model Posteriors For Set 2 σ_s.

Figure 2.9: Simulation Results of 300 Trials. 300 2IFC responses were simulated, and the resulting probability of each model for all participants are shown in the boxplot. Also shown are the probabilities with and without the cue conflict data for comparison.

Table 2.3
Model Classification of Simulated Set 1, Without CC Data.

		Winning Model		
Model Used	Trial Number	OPT	AVG	WTA
OPT	70	19	2	3
	140	18	0	6
	300	17	0	7
AVG	70	1	16	7
	140	1	21	2
	300	1	21	2
WTA	70	13	4	7
	140	12	2	10
	300	3	1	20

Table 2.4
Model Classification of Simulated Set 1, With CC Data.

		Winning Model		
Model Used	Trial Number	OPT	AVG	WTA
OPT	70	18	0	6
	140	23	0	2
	300	23	0	1
AVG	70	0	24	0
	140	0	24	0
	300	0	24	0
WTA	70	0	0	24
	140	4	0	20
	300	1	0	23

Table 2.5
Model Classification of Simulated Set 2, Without CC Data.

		Winning Model		
Model Used	Trial Number	OPT	AVG	WTA
OPT	70	17	5	2
	140	17	5	2
	300	17	7	2
AVG	70	12	9	3
	140	13	9	2
	300	11	13	0
WTA	70	1	5	18
	140	1	4	19
	300	0	2	22

Table 2.6
Model Classification of Simulated Set 2, With CC Data.

		Winning Model		
Model Used	Trial Number	OPT	AVG	WTA
OPT	70	14	5	2
	140	13	11	0
	300	18	6	0
AVG	70	9	15	0
	140	15	9	0
	300	3	21	0
WTA	70	0	2	22
	140	0	0	24
	300	0	0	24

2.6.1 Test-Retest Reliability Across Simulated Trials

Given that our experimental design involves blocks testing the same experimental condition (i.e. digit) on each of the two days, it is worth considering what

the distribution of the posterior will appear as when simulating σ across sets of trials. Thus, the responses of 24 participants to a 70 block set of 2IFC trials were simulated twice. The first and second set of 70 trials represent the first and second day of our testing experimentally. The 'digit' of each participant had an assigned set value of it's sensory acuity, which was drawn from a normal distribution $N(\mu = 1.0 \text{ mm}, \sigma = 0.3 \text{ mm})$ and held consistent for all trials. The comparison of each simulated participant's most likely σ in the first comparison against each other is shown in Figure 2.10. Note that the identity line, in red, is shown as a measure by which to compare the participant's performance across days 1 and 2. Similarly, the Bayesian confidence intervals (CI), which indicate here that there is a 75% probability that the true estimate lies within the interval, are included in the figure. The average σ value on the first set of 70 trials was 0.95 mm (SD = 0.28 mm) while for the second set it was 0.99 mm (SD = 0.28 mm). A paired t-test between the σ modes of the two blocks was conducted and found to be non-significant ($p = 0.17$). The simulation thus shows no significant difference between the two sets of results, as expected.

It should also be noted that even with an ideal participant, whose σ_s is not changed between trials, the responses display an unavoidable level of variability inherent to the task. The σ_s for each participant is not an exact match on each simulated day, as evidenced by the slight deviations from the identity line. Thus, this amount of variability is, at minimum, expected to also be present in human participants.

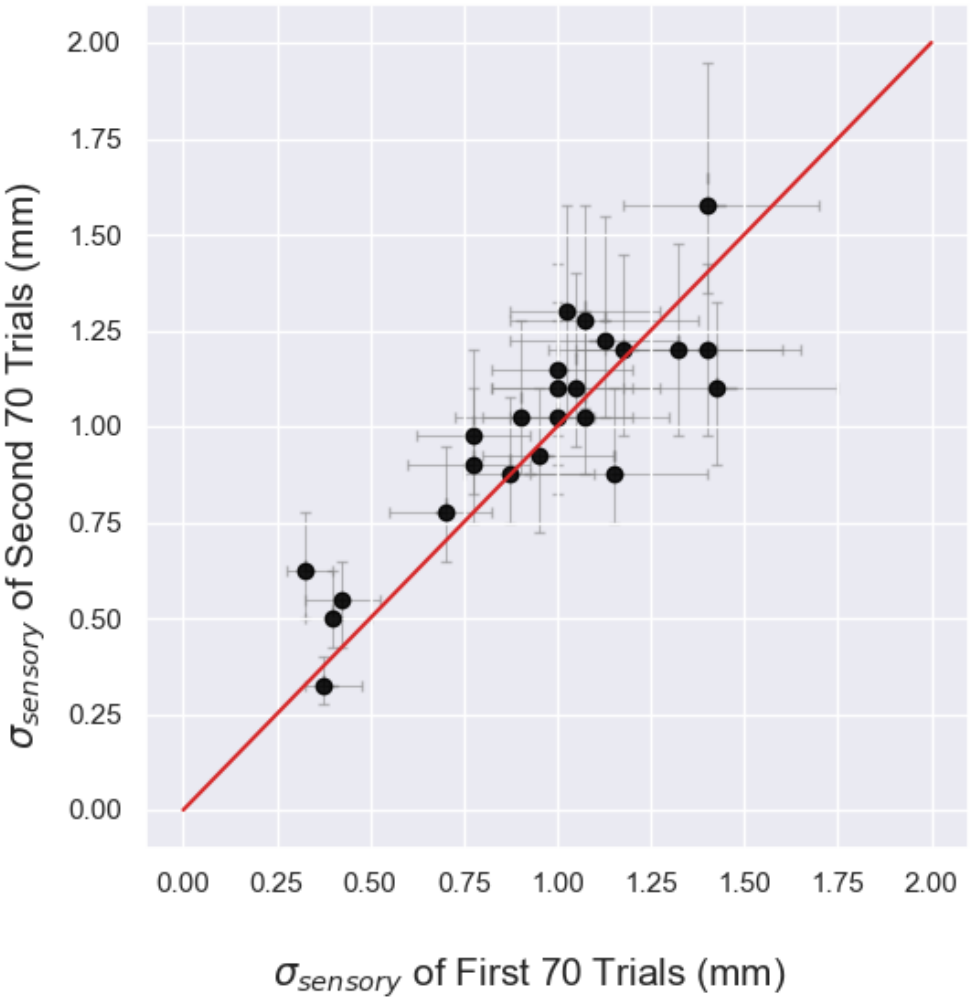

Figure 2.10: Comparing σ_s of Two Simulated Blocks. For each simulated participant, two blocks of 70 2IFC trials were produced and a resulting σ_s was generated. These two values are compared to each other in this figure, with an identity line in red for comparison, and the Bayesian 75% CI of each participant is present.

Chapter 3

Experimental Results

In this chapter we shall present both the methods surrounding the human participants and analysis of their results, drawing parallels to the analysis of the simulations performed in Chapter 2.

3.1 Methods

3.1.1 Participants

For this study 24 participants were recruited (mean age = 18.98, std = 0.78). Participants were recruited via the PNB Research Participation System (SONA) drawing from the McMaster University student body. Participants were screened via self-report for the following conditions, which can adversely affect tactile acuity or the ability to perform psychophysical tasks: diabetes, nervous system disorder or injury (tremor, epilepsy, multiple sclerosis, stroke, etc.), learning disability, dyslexia, attention deficit disorder, cognitive impairment, carpal tunnel syndrome, arthritis of the hands, hyperhidrosis.

3.1.2 Apparatus

For this experiment two multi-stimulus pieces were constructed. Each piece was designed using OpenSCAD and Ultimaker Cura software and printed in PLA plastic using an Ultimaker2GO 3D printer. The multi-stimulus piece consisted of a plastic bar with six edges protruding from it (see Figure 3.1a). Four of the six

edges were used in this experiment, and each edge was specifically designed to test either digit(s) D2, D3, D4 or D234.

The second multi-stimulus piece, which was designed for the cue conflict task of the last four blocks, consisted of a plastic cylindrical-like bar with 6 edges protruding from it (see Figure 3.1b). Each edge of this piece spanned all three digits. Four of the six edges were constructed as the reference stimulus for the respective four CC conditions, which were each labeled as either $-1.0, -0.5, +0.5$, or $+1.0$. The remaining two straight edges were constructed as the comparison stimulus, and were placed on opposite sides of the bar. The labelling of each CC condition reflected the position of the index cue edge relative to the middle cue edge. To elaborate, if the D2 cue edge position was more distal than the D3 cue edge the condition was denoted as a positive conflict ($'+'$), and conversely if the D2 edge was more proximal than the D3 cue edge the condition was denoted as a negative conflict ($'-'$). The magnitude of the condition (0.5 or 1.0 in mm) was reflected by the absolute value of distance of the D2 and D4 edges from the D3 edge. Of note is that the direction of the displacement of D2 and D4 edge were in opposing directions of equal magnitude.

The width of each stimulus edge piece was approximately 3 mm, and the length an edge spanning all three fingers was 80 mm. To ensure the digits were applied to only the edge of the stimulus that was appropriate two foam wedges were inserted between both D2 and D3 as well as D3 and D4.

In addition to the multi-stimulus pieces, a base piece was constructed to attach the stimulus piece to a stepper motor (ISM-7411 NEMA 23 National Instruments Integrated Stepper motor), allowing for a simple switch between the first and second multi-stimulus cue pieces (see Figure 3.2b). The multi-stimulus cue piece was mounted onto the base, and the base in turn was secured onto the stepper motor which rotated accordingly to change the stimulus level (Δ) applied to the participant. The stimulus level is applied through a custom computer program written in the LabVIEW (National Instruments) programming language. The LabVIEW SoftMotion module was utilized to control the stepper motor. Throughout the experiment the subsequent stimulus level was determined using a modified version Ψ method, which is a Bayesian Adaptive Procedure (BAP) created by Kontsevich

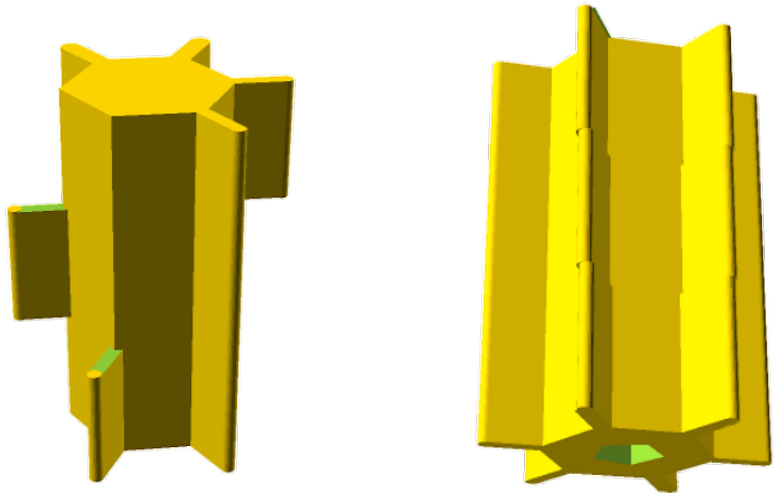

(a) (b)

Figure 3.1: Multi-Stimulus Cue Pieces. (a) depicts the non-conflict multi-stimulus piece used for the 2IFC in the first four blocks of the experiment while (b) depicts the CC multi-stimulus piece used for the last four blocks of the experiment.

and Tyler (1999). The BAP efficiently finds a participant's psychometric function by determining the most informative next stimulus intensity (Δ) to administer to the participant in order to maximize the information gained from their response. We modified this procedure by including a series of possible lapse rates, and later marginalizing over them, rather than assuming the lapse rate to be 0.04 as was done by Konsevitch and Tyler.

A hand rest for the participant was also developed, with three versions printed to accommodate the range of hand sizes present in the participant population (see Figure 3.2a). The posts protruding from the piece were intended to fit the crevices between D1 and D2 as well as between D4 and D5. A knob was attached to the center of the piece at the end facing the cue stimulus in order to slightly elevate D3. This was to ensure that with the movement of the fingers all digits would be relatively level with each other, as otherwise D3 has a tendency to extend further than D2 and D4.

A cardboard box was constructed to ensure that participants would not see the location of the stimulus edge. The box had two openings, a smaller one facing

the participant for them to place their hand within and a larger one in the back which the investigator could use to observe the participant's hand and the stimulus apparatus. The length of the participants forearm rested on a foam pad while their hand lay on the hand rest.

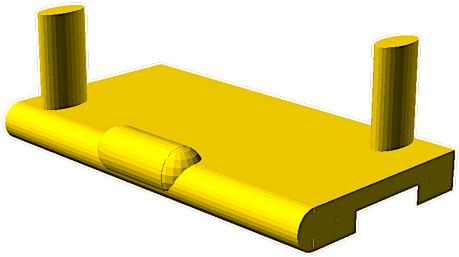

(a) Hand Rest.

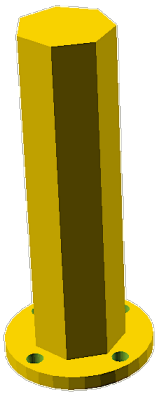

(b) Stimulus Support Base.

Figure 3.2: Support Pieces. (a) provides a depiction of the hand rest. D1 and D5 were placed on the outside of the two posts and D2, D3 and D4 rested in the center of the apparatus, with D3 resting on the rounded protrusion. (b) shows the base that the multi-stimulus cue pieces were placed onto. The flat circular disk was permanently attached to the stepper motor plate through the four screws-holes shown.

3.1.3 Procedure

Participants came in for testing over two days within a week from each other and on both days they were asked to complete the same task and in the same order. Upon beginning the experiment they were asked to sit down and place their hand in the appropriate position within the cardboard box. Recorded instructions were then played aloud and restated by the participant. To ensure their performance on the task would proceed smoothly they completed 30 practice trials of the 2IFC task, and during each trial of the practice automated auditory feedback on their accuracy was given. An infrared laser beam was present throughout all trials and used to ensure that the participants did not touch the stimulus outside of the appropriate time points. If the beam was broken, indicating that the participant's hand was touching the piece at an inappropriate time, an automated

computer voice instructed the participant to raise their hand. Once the practice trials were completed participants began the experimental blocks. Participants were not blindfolded during the study, as previous studies have indicated that doing so reduces performance on tactile tasks Zuidhoek et al., 2004.

On each day participants underwent 8 blocks of the 2IFC, with each block consisting of 70 2IFC trials. The first four blocks each individually tested either D2, D3, D4 or D234 while the last four blocks tested only D234 while applying each of the four possible CC conditions ($-1.0, -0.5, +0.5$, and $+1.0$). On each 2IFC trial the participant heard two auditory beeps (one for each interval) which indicated that they should tap their digits down onto the stimulus piece. They were tasked to compare the edge location on the first tap with the second, and state whether they believed the second edge to be proximal or distal relative to the first. Participants recorded their response by pressing the corresponding arrows on a USB remote. Between each block the participant was given a 2 minute resting period, with an extended break after the 4^{th} block. During this extended break the participant was led into another room to wait while the investigator removed the first multi-stimulus piece to then replace with the CC multi-stimulus piece, all without the participant's awareness. This swap was undisclosed to the participant in order to maintain the illusion that the participant touched only straight edges.

The order of the first four blocks was partially counterbalanced such that each of the six possible permutations of D2, D3, D4 was applied to an equal number of participants. The D234 condition was applied on either the first or last block, to an equal number of participants. The order of the last four blocks was also counterbalanced with 2 permutations, with respect to the direction of the CC (beginning either with + or − conflict). While ideally this study would be counterbalanced in 8! permutations, that would involve a sample size of 40320 participants. In total each of the 24 participants were given an order of the conditions which was unique to them.

3.1.4 The Guessing Bayes Factor

It was worth ascertaining whether participants did not pay attention or were guessing their responses. The guessing Bayes factor serves as a measure of the likelihood

ratio, which assesses the likelihood of the data given two hypotheses: one where the participant is making random guesses and another where the participant's responses follow a psychometric function, Ψ.

$$BF = \frac{P(Data|Chance)}{P(Data|\Psi)} \tag{3.1}$$

The numerator of this Bayes factor (Equation 3.1) calculates the probability of the participant's data (comprising both correct and incorrect responses across stimulus levels) assuming the participant is merely guessing (with a 50% chance of guessing correctly) on all trials up to the current one. On the other hand, the denominator computes the probability of the data based on the computer program's estimate of the participant's most-probable psychometric function. In the majority of cases, the guessing Bayes factor for the participant tends to converge towards zero as the experiment progresses from trial to trial, indicating that the participant's performance aligns with a psychometric function. However, we did find one participant who, on their day 1 D234 task, had a Bayes factor of 10, indicating they were likely guessing or inattentive on that block. Thus their data were removed from the analyses where appropriate.

3.2 Statistical Analysis

We performed paired two-tailed t-tests and repeated measures analysis of variance (RM-ANOVA) using python, with an α-level of 0.05. If the results indicated that RM-ANOVA failed Mauchly's test of sphericity then the Greenhouse-Geisser correction was used. Bonferroni adjustments were used for all main effect pairwise comparisons. The σ_s and μ values being analyzed represent the mode of the posterior probability distributions for each participant.

To begin the analysis we will focus only on the data from the non-conflict cue combination task conducted on the first four blocks of the study. Subsequently the results of the last four blocks, in which a cue conflict was applied, will be added to the data analysis.

3.2.1 Results of Non-Conflict Cue Combination

The first result of our analysis which was examined was the relationship between the results of the σ_s found on day 1 and on day 2. In Figure 3.3 the values of these results on day 1 and day 2 are plotted against each other, with an identity line present for reference. A further measure of comparison was conducted through paired t-tests on each digit condition. Comparing the day 1 and day 2 we find the results to be non-significant except for the condition of D234, where $t(22) = 2.26$ and $p = 0.03$ (uncorrected for multiple comparisons). Thus indicating that participants were consistent in their acuity D2, D3 and D4 but improved upon their acuity of D234 on the second day of testing.

Figure 3.4 summarizes the distribution of the σ_s values of each digit(s) on both days 1 and 2. The means and std of these distributions are also summarized in Table 3.1. Both of these results indicate that on day 1 the σ_s's of participants are lower for the individual digits (D2, D3 and D4) than for D234. In other words, acuity in the D234 is lower compared to the individual digits. Conversely, on day 2, it appears that there is no significant difference between all four of the conditions, such that D234 is neither significantly improved nor worsened compared to any digit by itself.

Table 3.1
The Average σ_s Value of Each Digit(s)

	D2 (mm)	D3 (mm)	D4 (mm)	D234 (mm)
Day 1 σ_s	1.73 (SD=0.81)	1.95 (SD=1.04)	1.50 (SD=0.73)	2.44 (SD=1.15)
Day 2 σ_s	1.70 (SD=0.88)	1.75 (SD=1.03)	1.51 (SD=1.04)	1.72 (SD=0.89)

RM-ANOVA on the σ_s values for day 1 confirms this, with $F(3, 69) = 5.9219(p = 0.004), \eta^2 = .099$. Mauchly's test indicated that the assumption of sphericity had not been met, $\chi^2[5] = 14.38\,(p = 0.013)$, thus the Greenhouse-Geisser estimates of sphericity, $\epsilon = 0.71$, correction was used for the analysis.

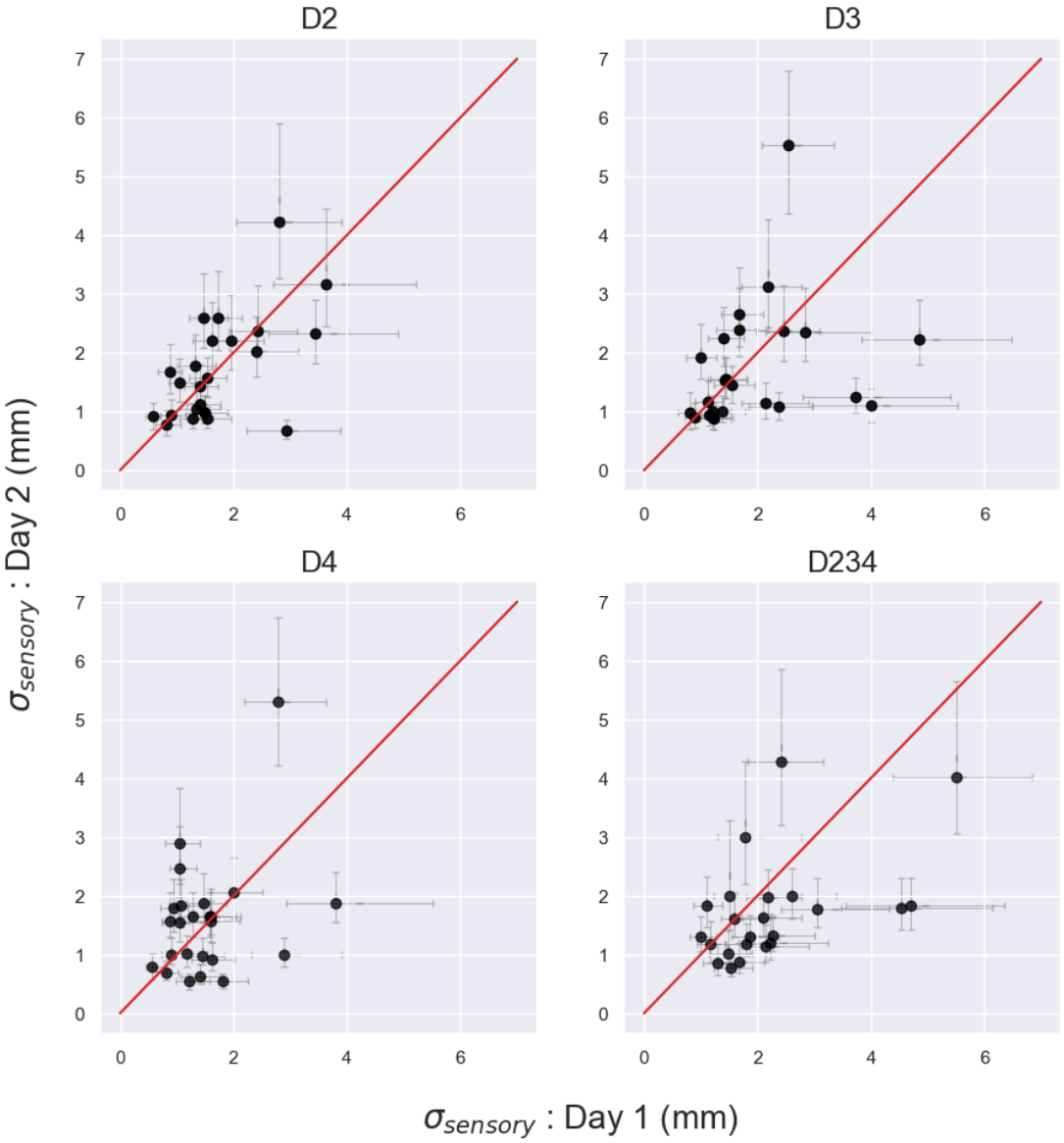

Figure 3.3: Comparison of σ_s on Days 1 and 2. The comparison for each digit's σ_s is shown for all participants. The red line serves as an identity line for reference, and the error bars represent the Bayesian 75% CI.

Post-hoc pairwise comparisons with a Benjamini/Hochberg FDR adjustment indicated that there was no significant difference between the σ_s values at the level of D2 and D3, ($p = 0.32$), at the level of D2 and D4 ($p = 0.25$) and at the level of D234 and D3 ($p = 0.12$). However, the σ_s value was was significantly higher at level D234 than at levels D2 ($t(23) = 2.57, p = 0.017$) and D4 ($t(23) =$

$3.30, p = 0.018$). A significantly higher σ_s was also found at the level of D3 than at level D4 ($t(23) = 2.94, p = 0.007$).

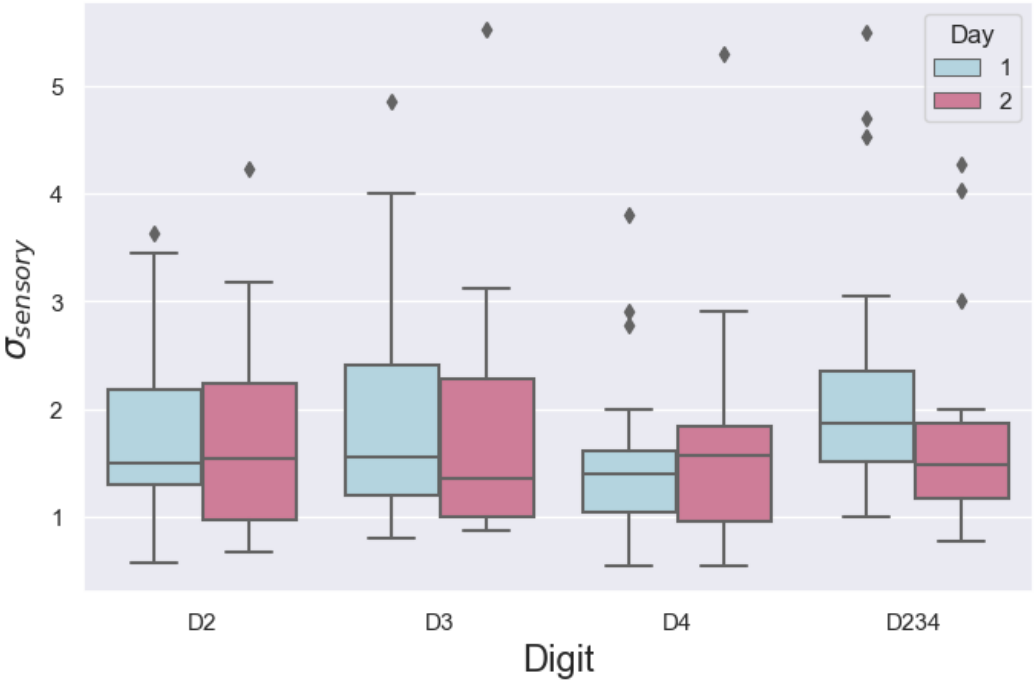

Figure 3.4: σ_s Posteriors for D2, D3, D4 and D234. The boxplot distributions of of σ_s are shown, such that the box shows the quartiles of the data set while the whiskers extend showing the rest of the distribution. The line in the box represents the median and outliers are indicated.

The same analysis was computed on day 2, and Mauchly's test indicated that the assumption of sphericity had been met $\chi^2[5] = 8.70\,(p = .120)$ and thus no correction was made. The effect of digit was not significant, $F(3, 69) = 0.74\,(p = .53)$, $\eta^2 = .010$ thus indicating that the D234 condition had a sensory acuity that was similar to D2, D3 and D4.

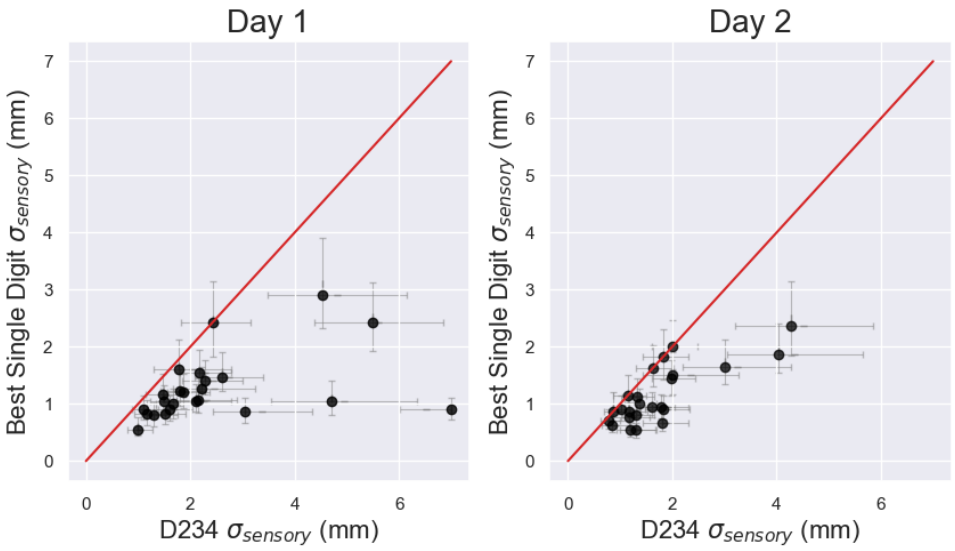

Figure 3.5: Best Single Digit vs D234 σ_s. This figure depicts the smallest (i.e. best) σ_s of the three individual digit against the σ_s of D234 on days 1 and 2. In this figure we see the general trend of the the best individual finger σ_s being less than that participant's D234 σ_s.

Another point of interest is determining how the finger with best acuity (lowest σ_s) compares to the D234 condition. In Figure 3.5 this comparison is mapped out on day 1 and day 2, with an identity line for reference. Paired t-tests for day 1 show $t(23) = -5.08\,(p < .001)$ indicating that the D234 condition is significantly worse in acuity than the individual's best finger. For day 2, similarly significant results were found with $t(23) = -5.01\,(p < .001)$.

Comparing the result of the observed D234 σ_s against what would have been predicted by the calculations of our models (see Table 2.1 for the method by which sigma was calculated) we can also gain a sense of how well these models are predicting the experimental data. The results of this comparison are shown in Figure 3.6.

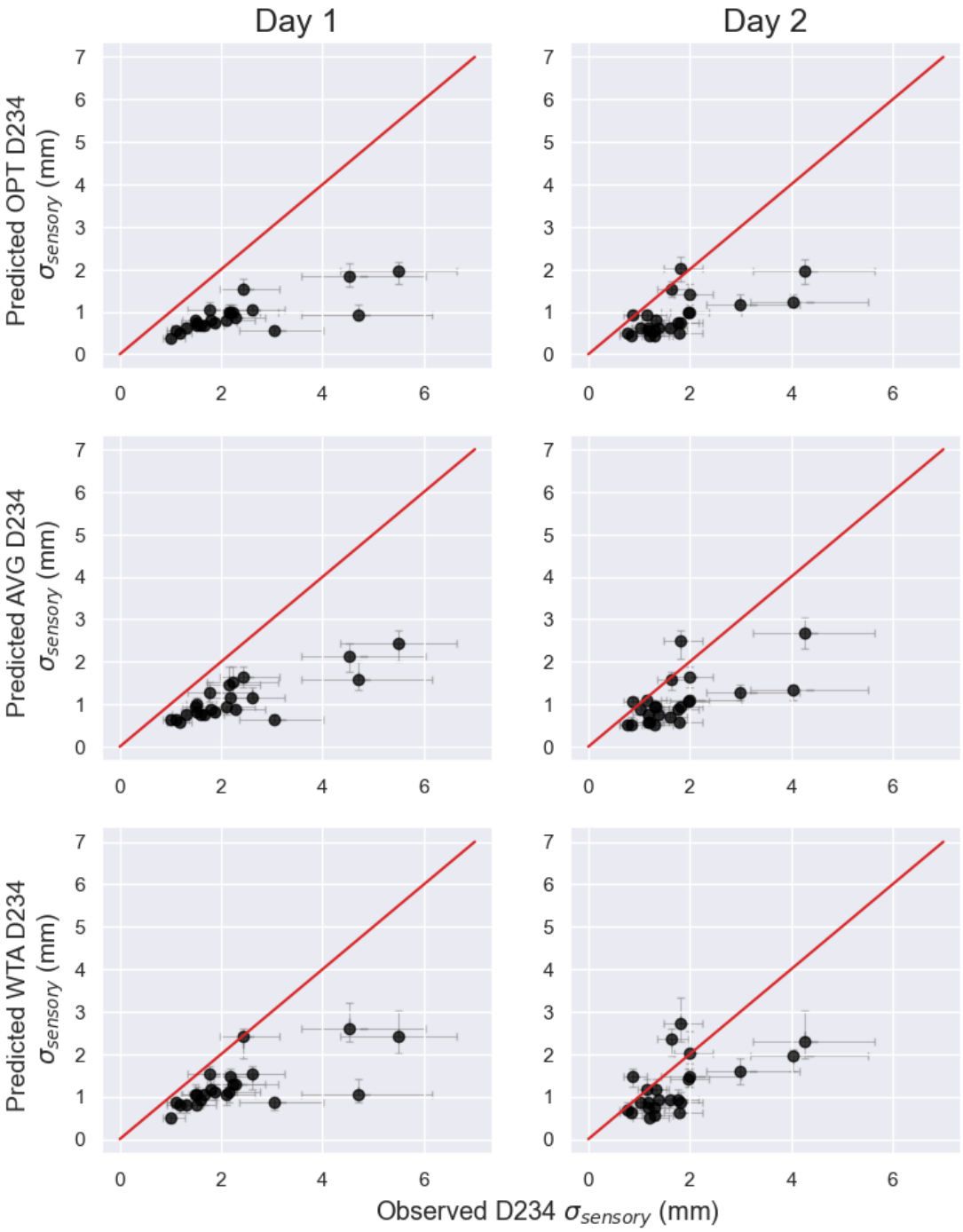

Figure 3.6: Observed vs Predicted D234 σ_s. For each participant the predicted D234 σ_s was calculated based on their D2, D3 and D4 psychometric functions and depicted against the observed D234 $sigma_s$ in laboratory on days 1 and 2. The identity line serves as a reference for how the two values compare.

More formally, in a paired sample t-test we see that on day 1 the predicted OPT, AVG and WTA D234 σ_s were all significantly lower than the experimental experimental D234 σ_s, with t(23) = -6.84 ($p < .001$), t(23) = -6.85 ($p < .001$) and t(23) = -5.07 ($p < .001$). Similarly on day 2 all D234 σ_s values predicted by models were also significantly lower, with t(23) = -6.74 ($p < .001$), t(23) = -4.12 ($p = .004$) and t(23) = -3.32 ($p < .001$).

These results appear to indicate that the current models we have present are not accurately capturing the data. Furthermore, given the lower than expected acuity present in D234, that there may be some other, as yet unstated, model currently utilized by observers.

3.2.2 Alternative Models

In order to make sense of the previous section's results we began to consider three additional models for the data. In a similar vein to the WTA model, in which the digit with the best sensory acuity is the only sensory cue used to determine the percept, the alternative models consist of a index-take-all (ITA), middle-take-all (MTA) and ring-take-all (RTA) models. Under these new models during cue combination only one digit forms the sensory percept, regardless of whether that digit has the highest acuity or not.

To determine whether these models were substantial we plotted the D234 σ_s against each individual D2, D3, and D4 σ_s for days 1 and 2 (see Figures 3.7 - 3.9).

To describe these figures paired t-tests were applied to the data points in each graph. For day 1, it was found that D2 and D4 had significantly better acuity than D234, $t(23) = -2.63\,(p = 0.011)$ and $t(23) = -3.94\,(p < .001)$ respectively while D3 did not differ significantly from D234 ($p = .105$). On day 2, it found that the acuity of D2, D3 and D4 all did not differ significantly from D234, where $p = .873$, $p = .881$ and $p = .216$ respectively. The relationship between these models seems especially fitting on day 2, increasing our belief that these models may be more descriptive of the data than those we had initially.

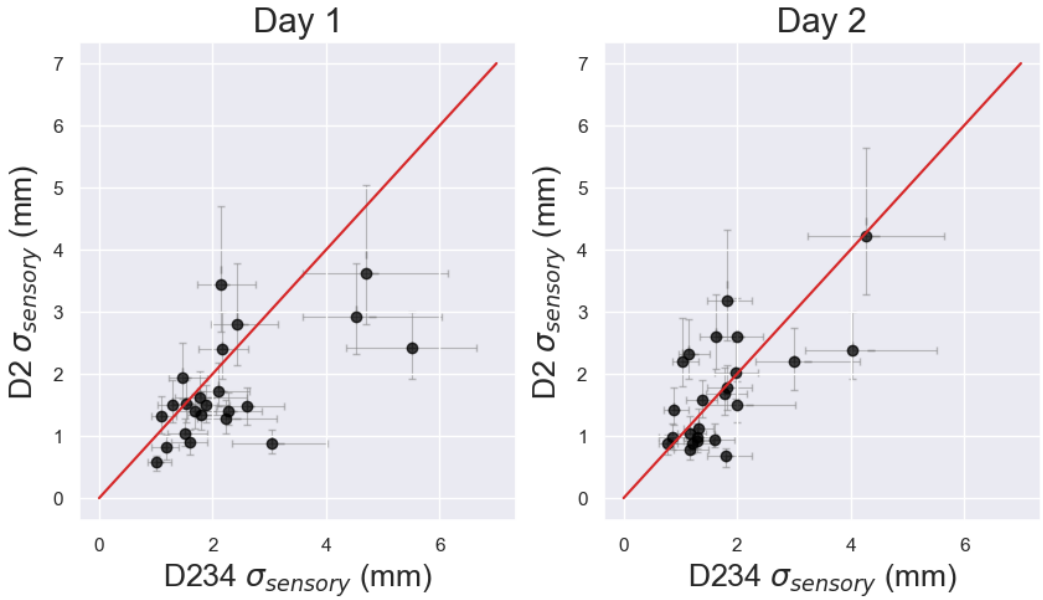

Figure 3.7: D234 vs D2 σ_s. Each day was shown comparing the observed D2 σ_s against the observed D234 σ_s with an identity line for comparison. The 75 % Bayesian CI of each σ_s value is also indicated, as well as an identity line in red.

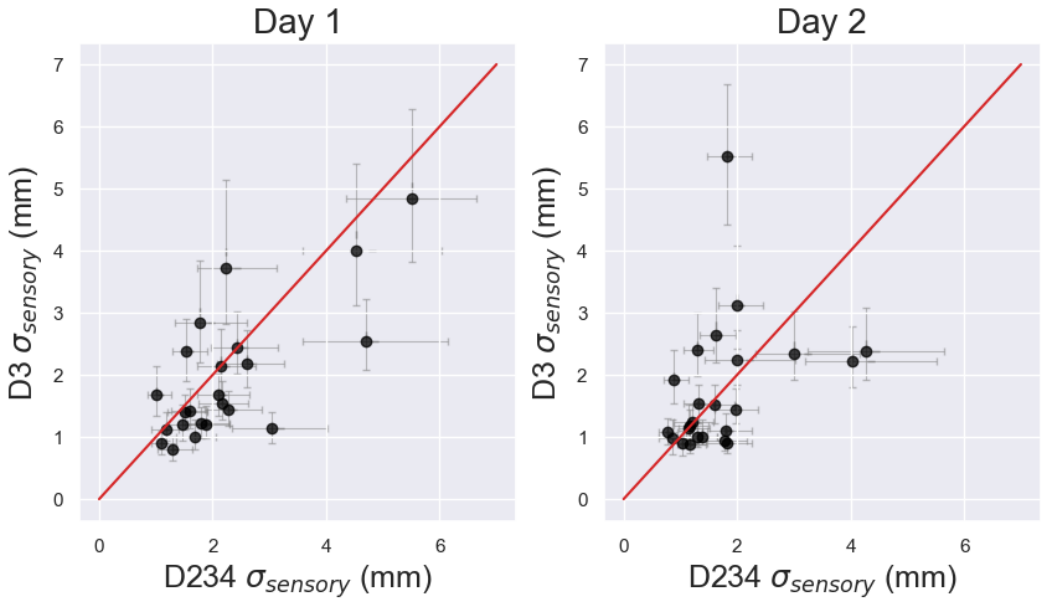

Figure 3.8: D234 vs D3 σ_s. Each day was shown comparing the observed D2 σ_s against the observed D234 σ_s with an identity line for comparison. The 75 % Bayesian CI of each σ_s value is also indicated, as well as an identity line in red.

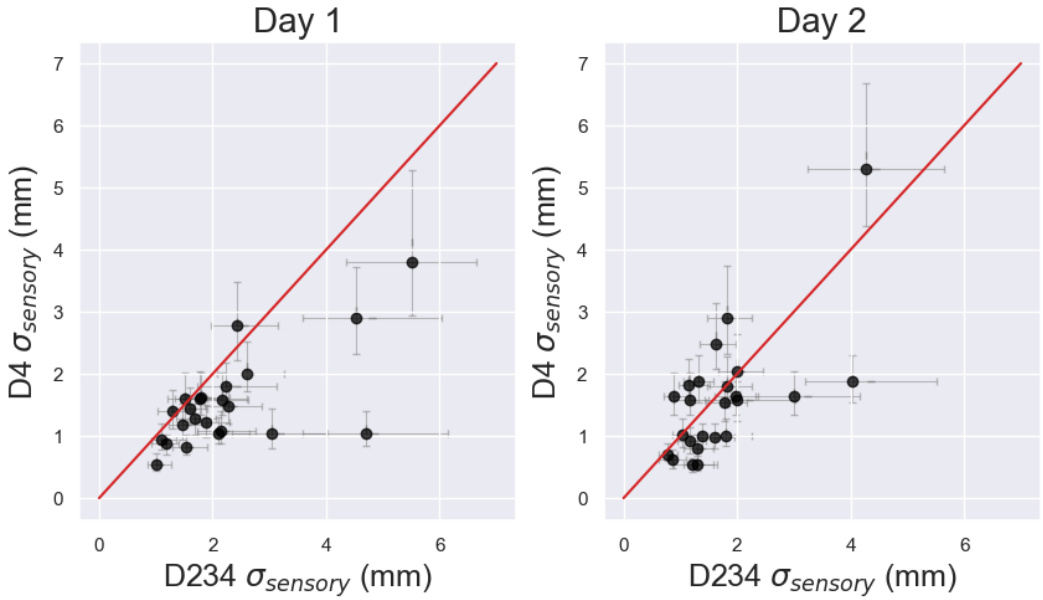

Figure 3.9: D234 vs D4 σ_s. Each day was shown comparing the observed D2 σ_s against the observed D234 σ_s with an identity line for comparison. The 75 % Bayesian CI of each σ_s value is also indicated, as well as an identity line in red.

3.2.3 Model Comparison without Cue Conflict Data

The final step for the analysis of the non-conflict cue combination data is to find the probability, using Bayesian inference, that the participants are using a particular model given their data. The results of these posterior probabilities are summarized in Figure 3.10 and the individual winning results in Table 3.2.

In Figure 3.10 the distributions on day 1 seem heavily skewed towards the alternative models, with ITA, MTA and RTA having similar ranges of probabilities, while the original models are less favoured. This distribution is also reflected in the results of Table 3.2, with the ITA, MTA and RTA being each chosen as the best model of 7 participants. On day 2 the more likely models appear to be shifted further towards the original three models in comparison to day 1.

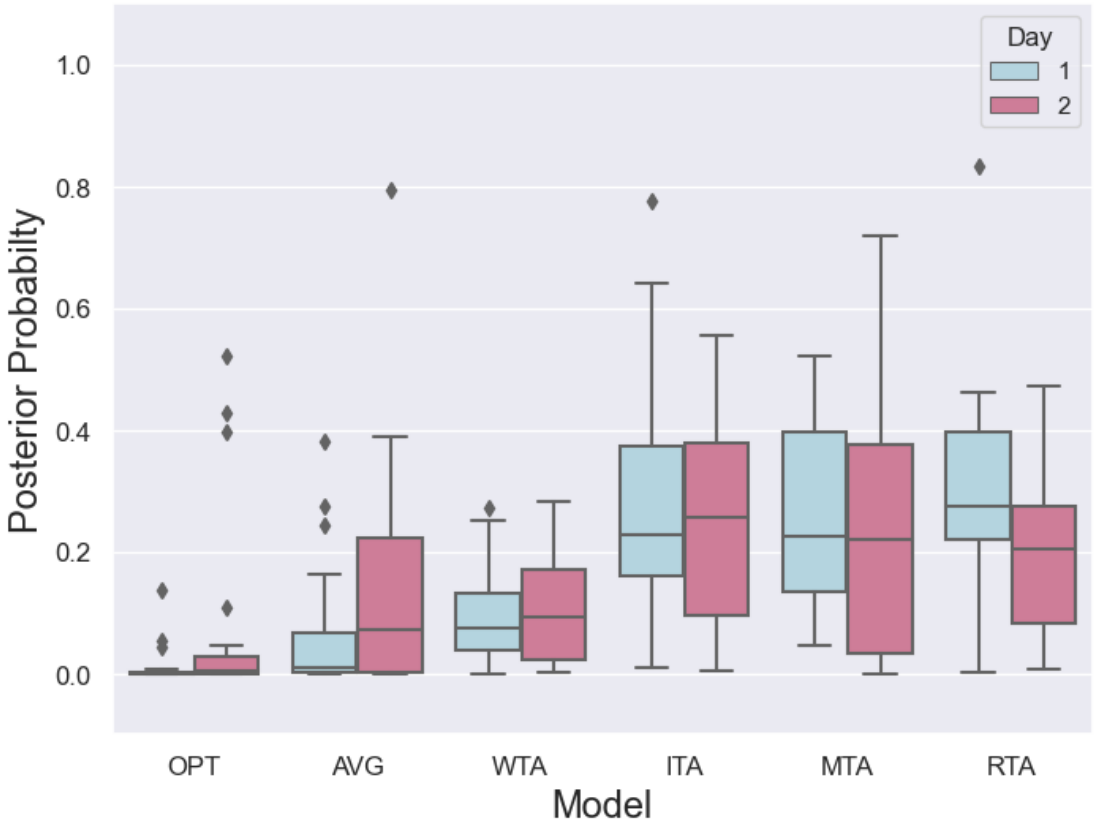

Figure 3.10: Model Posteriors, No CC Data. The boxplot distribution of the posterior probabilities of each model is shown, calculated while including the additional models. Results of each day are shown separately.

Table 3.2
Categorization of Each Participant's Model, Excluding CC Data

	Winning Model					
	OPT	**AVG**	**WTA**	**ITA**	**MTA**	**RTA**
Day 1	0	1	2	8	6	7
Day 2	3	2	3	9	7	0

3.2.4 Cue Conflict Data

As mentioned before, the prior analysis did not consider the data gathered from the cue conflict portion of the study, which will be this section's focus. As was

done for the participant's σ_s we can calculate the most likely perceptual bias μ for each CC condition. Figure 3.11 shows these values for each participant compared across the two days, with an identity line for reference.

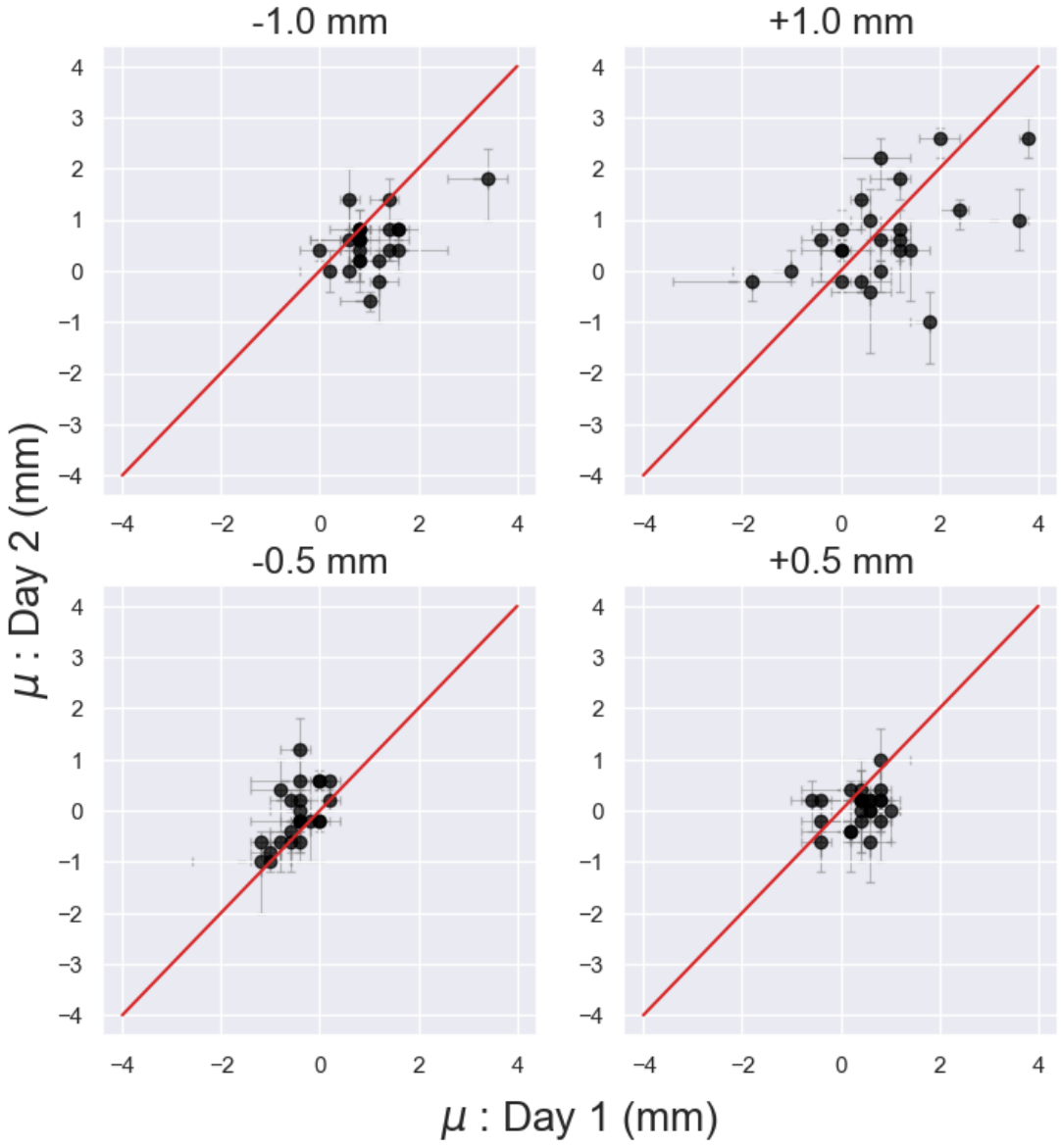

Figure 3.11: μ on Day 1 vs Day 2. For each cue conflict condition, a comparison of the the participant's day 1 and day 2 PSE shift, μ, is shown. Also present is an identity line in red for comparison and 75% confidence interval bars.

Conducting paired t-tests on the data in the figures we see that only for the +1.0 condition was found to have a non-significant p-value $p = .463$ while the other conditions, -1.0 , -0.5, +0.5, were all found to have significant difference. The values of the t-tests were $t(23) = 3.94(p < .002)$, $t(23) = -3.88(p < .001)$ and $t(23) = 3.30(p = .003)$ respectively. This shift in perceptual bias experienced by participants across days was unexpected and notable and is consistent with the idea that participants are, across days, changing the strategies they are using for cue combination.

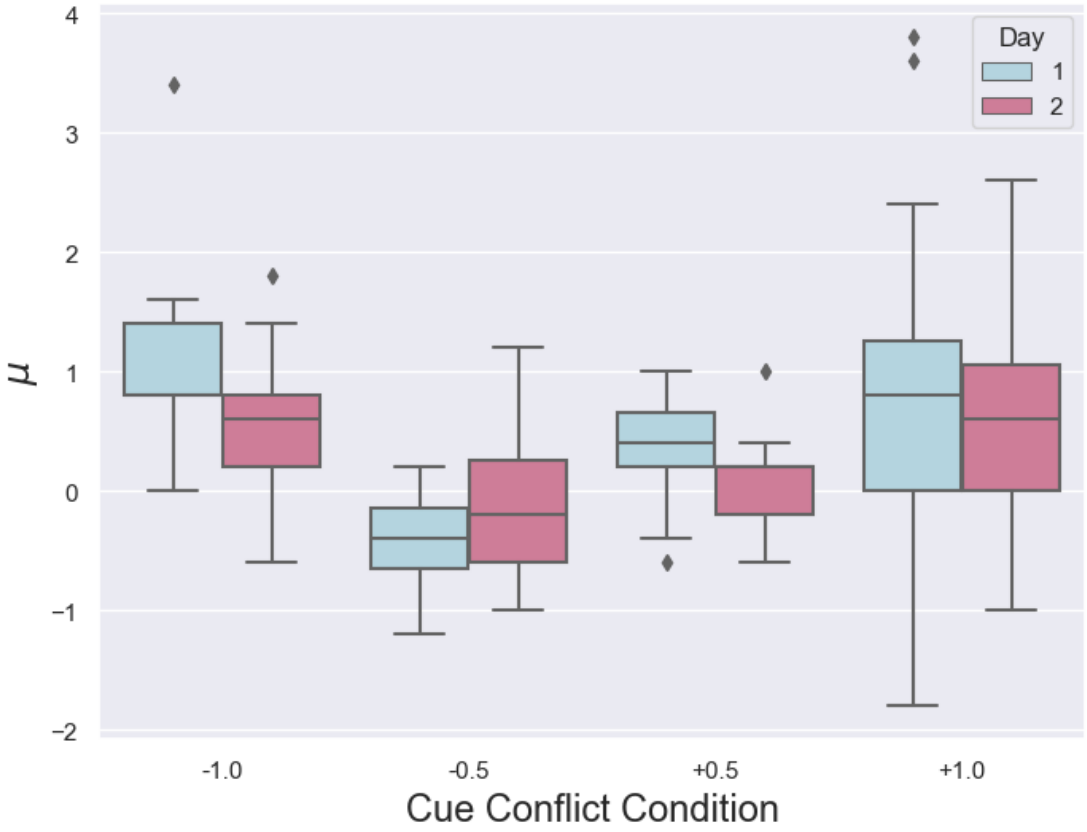

Figure 3.12: CC μ Distribution. The boxplots here show the distribution of μ values for each cue conflict condition on days 1 and 2, after adjusting for the various technical issues causing bias. The day 1 CC condition -1.0 median and day 2 +0.5 CC condition median coincides with the top line of the quartile box.

The distributions of μ values for each participant are shown in Figure 3.12 and highlight the difference across days 1 and 2, as well as across CC conditions.

The mean values for μ on each condition and day are listed in Table 3.3. At a glance, it appears that, on day 1, conditions -0.5, +0.5 and +1.0 support either an ITA model or a model where D2's σ_s plays a larger influence on the precept. Conversely while the -1.0 condition supports a RTA model or a model in which D4's σ_s significantly influences the percept. On day 2, this distinction appears less clear and seems to mostly support either an AVG model, an OPT model or a MTA model.

Table 3.3
The Average μ per CC Condition.

	-1.0	-0.5	+0.5	+1.0
Day 1: μ	1.04(SD=0.64)	-0.45(SD=0.40)	0.38(SD=0.43)	0.88(SD=1.24)
Day 2: μ	0.55(SD=0.51)	-0.09(SD=0.56)	0.06(SD=0.35)	0.70(SD=0.9)

A RM-ANOVA on day 1 μ values found a significant effect of CC condition, $F(3, 69) = 24.13\,(p < .001), \eta^2 = .369$. Mauchly's test indicated that the assumption of sphericity had not been met, $\chi^2[5] = 25.02\,(p < .001)$, thus the Greenhouse-Geisser estimates of sphericity, $\epsilon = 0.56$, correction was used for the analysis. Post-hoc pairwise comparisons with a Bonferroni adjustment indicated that there was no significant difference between the μ values at the level of +1.0 and -1.0, ($p = 0.47$) but significant differences (with all $p < 0.001$) at every other level. μ values in condition +1.0 were found to be significantly higher than those in +0.5 ($t(23) = 2.05$) and -0.5 ($t(23) = 5.05$) and similarly μ values in condition -0.5 were significantly lower than those in -1.0 ($t(23) = -11.66$) and +0.5 ($t(23) = -7.31$). Finally, values in condition -1.0 were significantly higher than those in condition +0.5 ($t(23) = 5.27$).

A RM-ANOVA on day 2 μ values found a significant effect of CC condition, $F(3, 69) = 11.12\,(p < .001), \eta^2 = .369$. Like on day 1 the assumption of sphericity was not met, $\chi^2[5] = 30.93\,(p < .001)$, and the Greenhouse-Geisser estimates of sphericity, $\epsilon = 0.56$ was used. To further examine the differences of the RM-ANOVA post-hoc pairwise comparisons with a Bonferroni adjustment were

conducted. Values between conditions +1.0 and -1.0 did not differ significantly ($p = 0.424$) as well as between +0.5 and -0.5 ($p = .200$). Conversely, values in condition +1.0 were significantly larger than -0.5 ($t(23) = 3.38$, $p = 0.016$) and -0.5 ($t(23) = 3.38$, $p = 0.016$). At the level of condition -1.0, it was significantly larger than the levels of condition -0.5 ($t(23) = 4.83$, $p < .001$) and +0.5 ($t(23) = 6.38$, $p < .001$).

3.2.5 Model Comparison With Cue Conflict Data

We can now turn to conducting the analysis of model comparison on the full dataset available to us. Again this model comparison will include the three additional models, ITA, MTA and RTA. The distribution of posterior probabilities for results of the comparison are shown in Figure 3.13. On day 1 the models that appear to be the most favoured are AVG, WTA, ITA and MTA, while on day 2 the most likely models are AVG, WTA and MTA; notably the MTA model is in the lead for both days. On both days, the OPT and RTA model are not favoured.

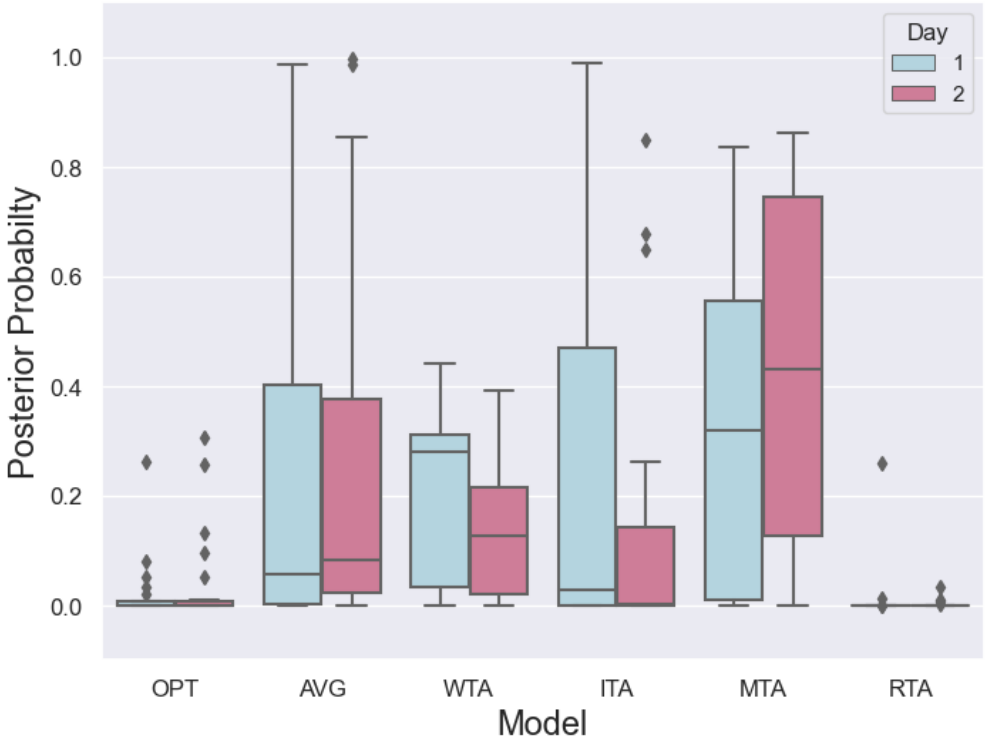

Figure 3.13: Model Posteriors, With CC Data. The Boxplots distribution of the posterior probabilities are present, where the probabilities are calculated using the CC data for days 1 and 2.

The final categorizations of each model are shown in Table 3.4, and seem to reflect the distributions from Figure 3.13. In these new analyses, the AVG, ITA and MTA are the only models that participants are being categorized as.

Table 3.4
Categorization of Each Participant's Model, Including CC Data.

	Winning Model					
	OPT	**AVG**	**WTA**	**ITA**	**MTA**	**RTA**
Day 1	0	6	0	8	10	0
Day 2	0	7	0	4	13	0

Chapter 4

Technical Considerations and Pilot Study

This chapter focuses on the technical aspects of our study, particularly those related to the cue conflict testing. During this examination, certain concerns emerged regarding the reliability of the cue conflict data and, consequently, our ability to interpret the results of our analysis. To address these issues, we conducted a new pilot study.

4.1 Questions About the Cue Conflict Condition

When we initially analyzed the cue conflict data, we observed an unexpected trend. On both days 1 and 2, there was a significant 'dip' in the data. Notably, the mean value (μ) for the -0.5 condition was -1.5 mm and -1.3 mm on the respective days. This raised concerns because these values were considerably larger than what we would anticipate given the experimental conditions. For instance, even if participants were using an ITA strategy, such a perceptual shift exceeded the true cue conflict introduced by the stimulus. This distribution is depicted in Figure 4.1, which can contrasted with Figure 3.12 for reference.

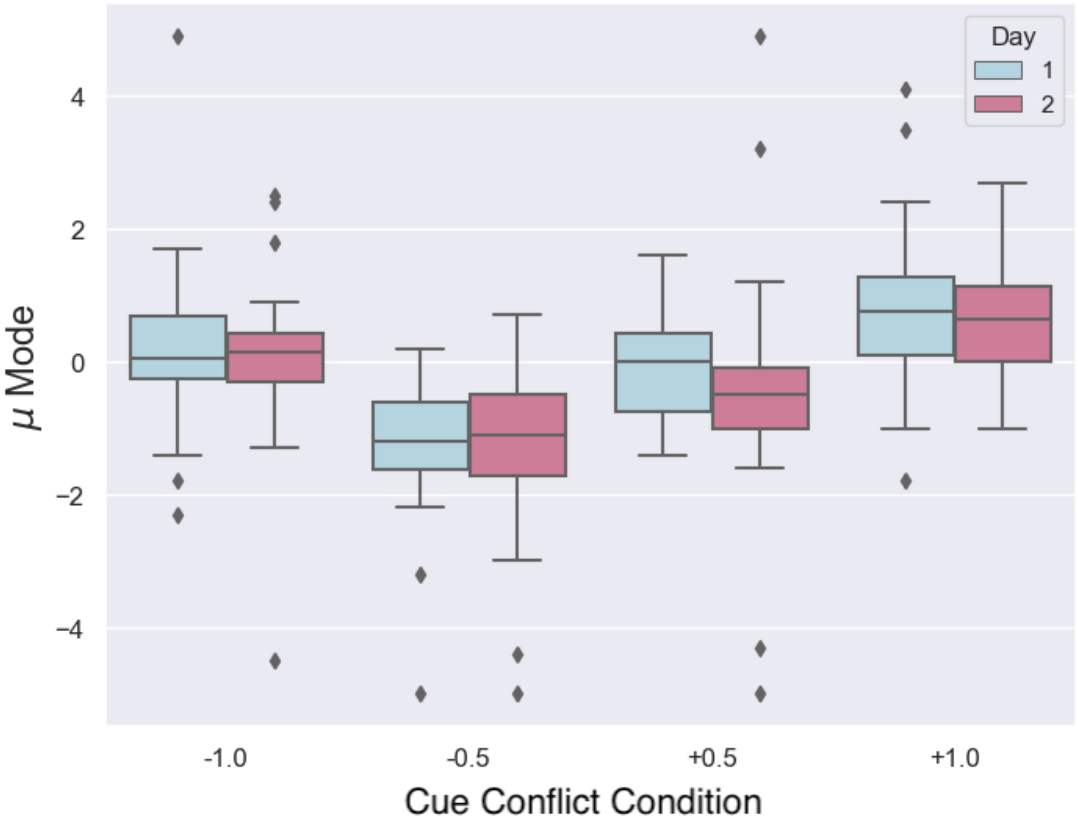

Figure 4.1: Original CC μ Distribution. Without making the relevant key adjustments, the distribution of the most likely μ values of each participant on days 1 and 2 appears as so. Of note is that on the -0.5 CC condition we see that the distribution of values is far lower than expected.

This prompted us to conduct a thorough investigation to understand the reasons behind this 'dip' in the data. Our investigation revealed several potential sources of error, which, in turn, enabled us to refine our final analysis. In Chapter 3, we presented the outcome of this recalibration process, and will shortly outline the steps taken to arrive at what we consider to be a more accurate result.

4.1.1 Cue Conflict Multi-Stimulus Piece

Our investigation began by scrutinizing the cue conflict multi-stimulus piece itself to identify any physical features that might explain the observed discrepancy.

Upon measuring the width of each edge of the stimulus piece, we discovered variations to exist between them. Despite the software specifications indicating a width of 3 mm for the cue piece, we found that for conditions +1.0, +0.5, -0.5, and 1.0, the average edge widths were 2.7 mm, 3.0 mm, 2.8 mm, and 3.1 mm, respectively. The two straight comparison edge widths were also 2.8 mm and 2.9 mm. In contrast, the average width of each edge in the normal cue combination stimulus consistently remained around within +/- 0.1 mm of 3.0 mm. The most likely cause of this discrepancy was attributed to challenges in the 3D printing process when producing the cue conflict multi-stimulus piece. Measures were subsequently taken to rectify this error in printings of the stimulus for future use.

While the difference in thickness may be relatively small, this could introduce a confounding variable in the results, as the process of model comparison assumes that the σ_s for each digit remains constant. However, if the stimulus edge changes it's width, this could mean that the participant's σ_s has changed and thus our analysis loses some power in its accuracy.

So while this may play some role in explaining the data, it does not, however, appear to be a full solution. As such, we looked to other possibilities to explain the data.

4.1.1.1 Increasing Precision of the 3D Printer

Addressing the 3D printer-related issue entailed a substantial process of trial and error, during which multiple steps were implemented to produce a refined stimulus piece devoid of the problems encountered in the original study's stimulus. One of the precision challenges stemmed from the fact that the cue conflict edges had to be printed with varying support stands beneath them, unlike straight edges. To enhance edge stability and sharpness, we reduced the print speed from 60.0 mm/s to 50.0 mm/s, allowing more time for each plastic layer to cool before the next one was added. Additionally, we increased the infill amount, representing the print's density, from 20% to 50% to provide enhanced structural support during the printing process. To further enhance print resolution, we adjusted the layer height from 0.1 mm to 0.06 mm. Lastly, the wall count layer, a measure of the outer wall thickness in terms of layers, was increased from 3 to 5, based on a layer

view analysis indicating that this adjustment would improve both the stability and resolution of the print design.

4.1.2 Home Position of the Cue Conflict Stimulus

In our exploration of the data, an issue was also discovered with the home position of the multi-stimulus CC piece. To explain, between the first four blocks and the last four blocks there is a change in the cue piece from the non-conflict multi-stimulus piece to the cue conflict multi-stimulus piece. As such, the cue conflict multi-stimulus piece would need to rotate into the correct position once the 5^{th} block began. However, it was discovered that while a 72° rotation would be required to accomplish this task, only a 60° rotation was done, leading the resulting cue piece to be, on a whole, 12° distal from its 'home' position on the digits. This reduces the accuracy of our analysis, as we assume the participant's σ_s for each digit to be consistent from the first half to the second. However, changing the position of the edge to such a large degree may also result in changing the participant's σ_s during their CC trials. As a result, assumptions made during our analysis of the participants' posteriors when including CC data may not be valid. Another unintended consequence of this issue is that the digits on the CC multi-stimulus were at times aligned incorrectly. It was reported by some participants that certain digits (particularly D4) could, at times, not feel the reference or comparison stimulus during some CC conditions.

4.1.3 Rotation of the Cue Conflict Edge

Subsequently, a more significant issue emerged during the investigation. A discrepancy was identified between the experimental distance programmed into the computer, which instructed the motor's rotation in each 2IFC trial, and the presumed distance between the comparison stimulus and the reference stimulus. Specifically, the computer directed the motor to rotate 60° from the middle cue edge on the reference (CC) stimulus to the straight edge of the comparison stimulus. However, laboratory measurements revealed that the rotational steps required to traverse this path differed from the expected 60°, and these discrepancies had implications

for our analysis. For conditions -1.0, -0.5, and +0.5, the differences were calculated to be 0.578 mm, 0.716 mm, and 0.405 mm, respectively, added in the distal direction. To rectify this issue in the analysis, these values were incorporated into the total distance moved by the comparison stimulus. It is worth noting that this disparity between the experimental and calculated stimulus levels may have compromised the efficiency of BAP, as the procedure relied on inaccurate stimulus intensities (i.e. Δ) to choose the next stimulus level.

4.1.4 Speculative Analysis

As previously mentioned, the home position of the CC multi-stimulus piece was shifted 12° distally. This adjustment occasionally led to a situation where the participants' shortest finger, typically D4, couldn't physically reach the stimulus. Such occurrences were primarily limited to specific CC conditions that positioned the edge of the shortest finger further distally.

The absence of this tactile cue was particularly relevant because it had the potential to influence participants' perception, making them perceive the cue as being more distal in the reference task than it actually was. Given that this issue was most likely to arise in the -1.0 CC condition, where the D4 edge was in the furthest distal position, we performed the same Bayesian analysis while excluding the data from this condition only.

The results are presented in Figure 4.2 and Table 4.1. These results indicate a slightly more pronounced inclination towards the ITA model on day 1, in contrast to the findings reported in Chapter 3. Meanwhile, the results for day 2 exhibit relatively consistent outcomes.

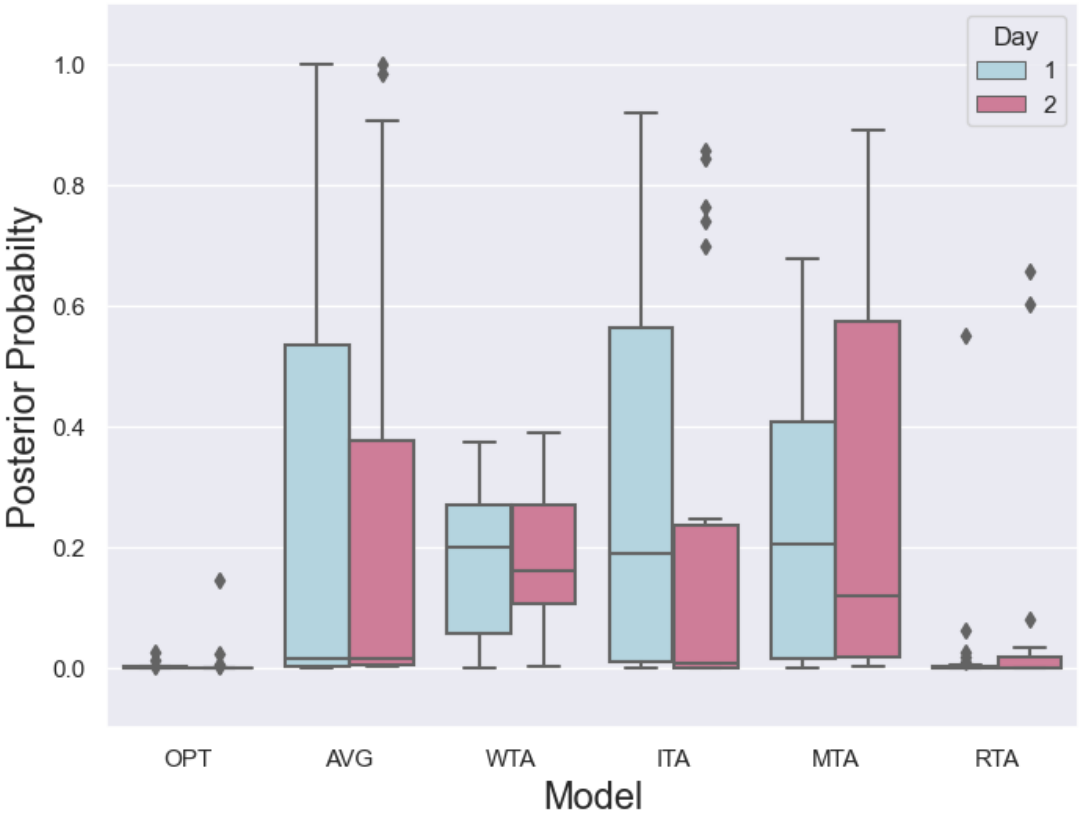

Figure 4.2: Model Posteriors, Excluding +1.0 CC Condition. In this figure the distribution of the posterior probabilities are shown, but are calculated without the CC condition +1.0 from the data on days 1 and 2.

Table 4.1
Categorization of Participants when Excluding CC Condition -1.0 mm from Data.

	Winning Model					
	OPT	**AVG**	**WTA**	**ITA**	**MTA**	**RTA**
Day 1	0	7	0	8	8	1
Day 2	0	6	0	5	11	2

4.2 Pilot Study

The goal of the pilot experiment was to construct a study which attempted to address the question raised by the original study, i.e. examining whether or not extended training would influence which models participants were most likely employ for cue combination. If participants do improve and 'switch' to more optimal models as a result of increased training, we will likely see a sensory D234 σ_s that is much lower than any other digit's sensory σ_s on day 5 in comparison to the participant's results on day 1.

4.2.1 Methods of Pilot Study

While the pilot study makes few changes to the 2IFC testing procedure of the original study, there are some key changes made to the overarching structure of the experiment which will be discussed in the following paragraphs. The apparatus and general laboratory organization also remains unchanged with regards to the original study. The exception to this were the cue pieces used for the 2IFC task, which were reprinted to remove the issues faced within the original study. The dimension of the cue pieces were also changed by decreasing the width from 3 mm to 2 mm. Three undergraduate participants were recruited from within our lab for this pilot, and they will be referred to as P1, P2 and P3.

The participants came in for testing over a 5 day period, and on day 1 and day 5 they completed the same procedure as the original study's day 1 and day 2. In other words, on the first and last day they completed 4 blocks of the non-conflict cue combination task (see Figure 3.1a for reference to the multi-stimulus piece used) and on the last four blocks they under went a cue conflict task (see Figure 3.1b for reference to the multi-stimulus piece used). Similar to the original study, each block consisted of 70 trials of the 2IFC task.

Days 2, 3 and 4 were dedicated to training the participants on the 2IFC task. On these days only the normal cue combination task (thus only the cue stimulus seen in Figure 3.1a) was used. To further examine whether the type of training had an affect, the participants were divided into two groups. One participant (P1)

only experienced the D234 edge stimulus for all training day blocks while two participants (P2 and P3) equally divided the blocks between the four edges (D2, D3, D4 and D234). While the pilot's sample size is small, we hope to expand on the between-subjects condition in a future study. Throughout all training days each participant received automated feedback indicating their correct/incorrect judgements of each 2IFC trial.

4.2.2 Preliminary Results of Pilot Study

Like in Chapter 3 of this thesis I will begin by contrasting the values of σ_s on day 1 and day 2 of the experiment. The results are shown in Figure 4.3 and indicate that while P1 did not differ greatly between days, P2 and P3 show some improvement in their acuity on day 5 across all four conditions.

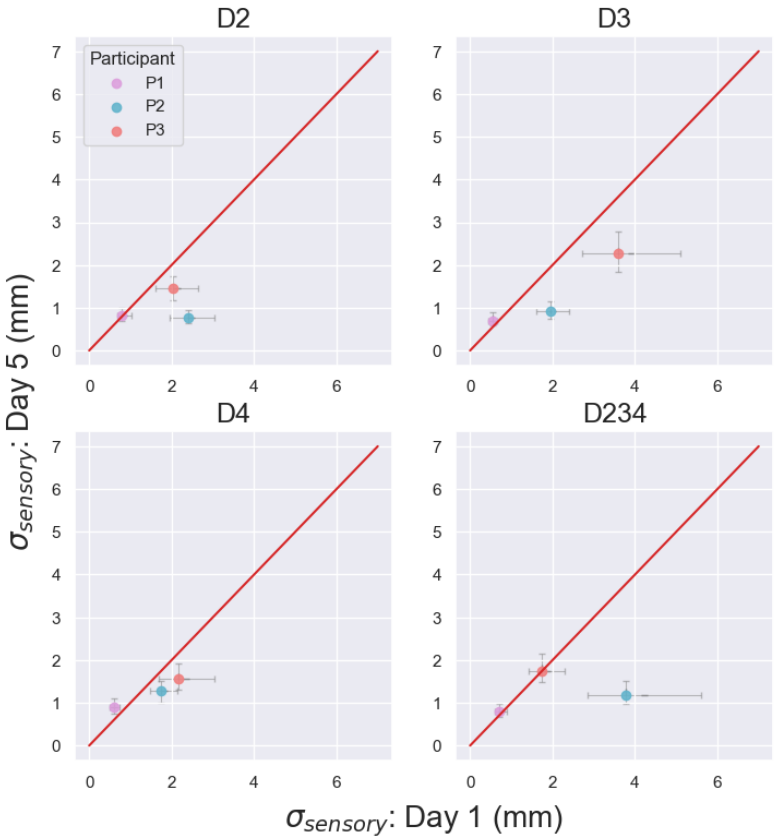

Figure 4.3: Pilot: Comparison of σ_s. The three pilot participants are distinguished by colour, and an identity line in red is present for comparison. The Bayesian 75% CI is shown as well.

In Table 4.2 the mode of the σ_s posteriors on days 1 and 5 are shown respectively, and appear to indicate that P1 and P3 did not show a pattern of greater acuity in D234 than all of their individual digits, and did not improve in reducing their σ_s greatly upon training. While P2 did show large improvements in their acuity of their D234 on day 5 compared to D1, their improvement was not to the extent that it was clearly better than any single digit.

The next step in the analysis was to apply Bayesian model comparison to find what model the participants are most likely using. The distribution of probabilities for each model is shown in Figure 4.5. No consistent trend was found among the three participants, but results here do seem to be consistent with the results of the original study in Chapter 3. On days 1 and 5, the ITA, AVG and RTA models have the largest posteriors, though participants 2 and 3 are classified under different models for the two days. The final classifications are shown in Tables 4.4 and 4.5, showing the calculations completed both with and without cue conflict data.

Table 4.2
Pilot: σ_s of Each Digit.

σ_s on Day 1					σ_s on Day 5				
ID	**D2**	**D3**	**D4**	**D234**	**ID**	**D2**	**D3**	**D4**	**D234**
P1	0.8	0.6	0.6	0.7	P1	0.8	0.6	0.9	0.8
P2	2.4	2.0	1.8	3.8	P2	0.8	0.9	1.3	1.2
P3	2.0	3.6	2.2	1.8	P3	1.4	2.3	1.6	1.8

Table 4.3
Pilot: μ of Each CC Condition.

μ on Day 1					μ on Day 5				
ID	**-1.0**	**-0.5**	**+0.5**	**+1.0**	**ID**	**-1.0**	**-0.5**	**+0.5**	**+1.0**
1	0.8	0.4	-0.8	0.0	1	-0.8	1.4	-1.2	0.2
2	-0.2	-1.0	-1.2	0.0	2	-2.0	-2.4	-0.6	-1.2
3	-0.6	-0.2	-0.2	0.0	3	0.0	1.2	0.4	0.8

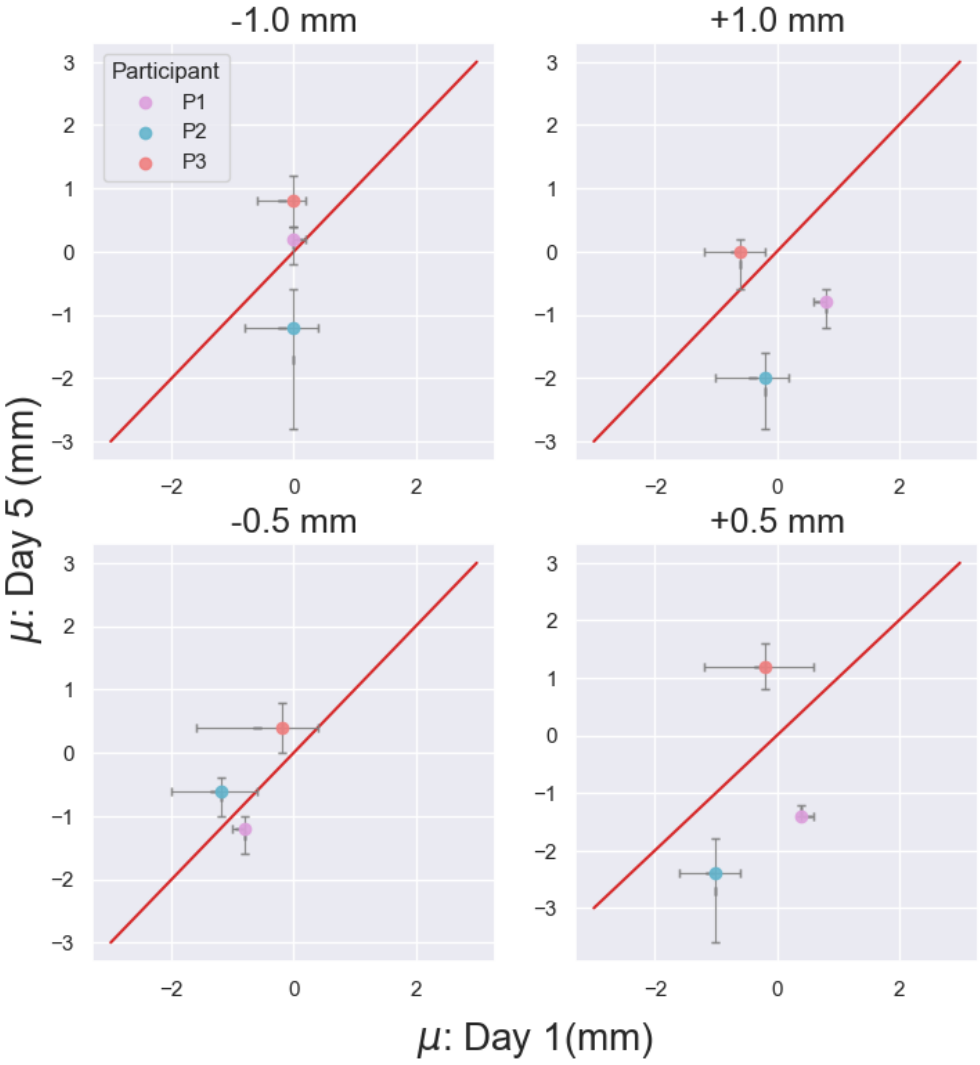

Figure 4.4: Pilot: Comparing μ on Days 1 and 5. The three pilot participants are distinguished by colour, and an identity line in red is present for comparison as well as the 75% Bayesian CI.

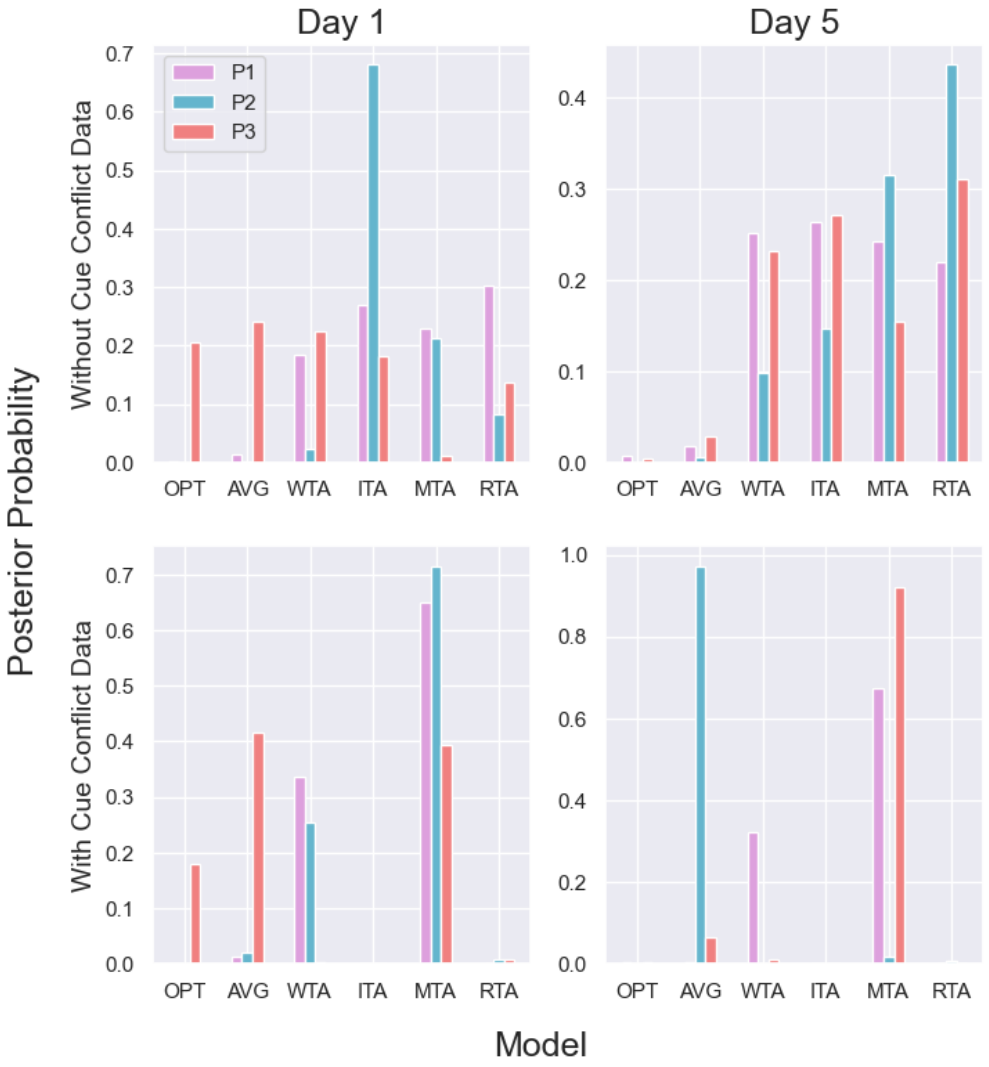

Figure 4.5: Pilot: Model Posteriors For Each Participant. The above distribution is of the posterior probabilities calculated for each model on days 1 and 5 of the pilot. The top row of figures shows the probability calculated without the CC data while the bottom row of figures shows the probability when including it.

Table 4.4
Pilot: Categorization of Each Participant's Model, Excluding CC Data.

	Winning Model					
	OPT	**AVG**	**WTA**	**ITA**	**MTA**	**RTA**
Day 1	0	1	0	1	0	1
Day 5	0	0	0	1	0	2

Table 4.5
Pilot: Categorization of Each Participant's Model, Including CC Data.

	Winning Model					
	OPT	**AVG**	**WTA**	**ITA**	**MTA**	**RTA**
Day 1	0	1	0	0	2	0
Day 5	0	1	0	0	2	0

Further investigation with a larger sample size of a naïve participant population will be necessary to determine whether the results of the pilot are representative. As is, the pilot data seems to suggest that training is not as effective in producing optimal cue combination as would be predicted given the results of the original study.

Chapter 5

Discussion

General Discussion

The general focus of this thesis centers on employing a Bayesian perceptual framework to further our understanding of tactile cue combination in human perceptual systems. Specifically, our goal was to investigate whether the brain optimally performs tactile multi-cue integration. Underscoring this framework was an understanding of the probabilistic nature of decision-making and the role of sensory noise in the sensory process. The human hand was chosen as a focus in our experimental design due to its relevance in tactile perception. Bayesian inference was described as a normative model of perceptual processes and applied to our understanding of how the brain constructs models of the external world and abstracts complex sensory inputs. The integration of multiple sensory cues was examined, and three models of cue combination (OPT, AVG and WTA) were initially presented as possible candidates.

Prior to testing participants in a laboratory setting, computer simulations were employed to simulate human participant responses, serving as reflections of expected outcomes in actual experiments and as proof of concept. The simulation settings mirrored the same testing procedure conducted in laboratory settings,

which involved a two-day experiment with eight blocks, each consisting of 70 trials of a 2IFC task. The computer program simulated 24 participant responses, drawing from two idealized distributions their sensory acuity (σ_s), and underwent each of the three models cue combination. The simulations showed the strength of Bayesian model comparison in correctly classifying the results, which increased in accuracy with both a larger number of trials and when cue conflict data was included.

The experimental study also involved 24 participants recruited from McMaster University, and various screening criteria were applied to ensure the participants' eligibility. Statistical analyses were performed, comparing participants' sensory acuity (σ_s) for each digit conditions on day 1 and day 2. The results showed that participants improved their acuity for D234 on day 2, while D2, D3, and D4 remained consistent. The analysis also compared participants' best single-finger acuity to D234 acuity and found significant differences, with the single-digit showing more sensitivity than D234. Additionally, participants' D234 acuity was compared to model predictions, revealing significant discrepancies. Alternative models, including index-take-all (ITA), middle-take-all (MTA), and ring-take-all (RTA), were considered as a result. These alternative models were shown to be a better fit for the data than the original three were alone. The analysis also incorporated cue conflict data, which showed a shift in perceptual bias between day 1 and day 2, particularly on conditions -1.0 , -0.5 and +0.5. Model comparison revealed that when cue conflict data is not considered, the ITA and MTA models are favoured on both days. When cue conflict data is considered, the MTA, ITA and AVG model were the most favored on both days, though ITA categorizations decreased by day 2.

During the initial stages of data analysis, concerns arose regarding the reliability of cue conflict data and its impact on our analysis. An unexpected dip in the data was observed, particularly in the -0.5 condition, prompting a thorough investigation into potential sources of error. Discrepancies in the CC multi-stimulus piece's physical features, 3D printing precision and rotation positioning issues were identified and addressed.

From the final results of the study it becomes clear that in this experimental

design tactile cue integration is markedly sub-optimal. The results of this study are in line with the previous work by our lab by Prodribaba (2018), in which participants also failed to achieve optimal cue combination of tactile cues. Similarly, a paper by Rosas et al. (2005) had also shown non-optimal cue integration of texture and haptic cues in participants. However, many other studies on cue integration indicate optimal cue integration, leading us to consider what could be the cause of this lack of optimally in our study Alais and Burr, 2004; Ernst and Banks, 2002; Körding and Wolpert, 2004.

Perhaps mediating this issue is a lack of experience in the experiment-specific task, which in turn is reducing the participants' ability to integrate sensory information on this task optimally. Within our study it appears that there is some improvement from day 1 to day 2, specifically in condition D234, indicating the possible role of training in moving the participants towards optimally (or towards being less sub-optimal). Of note, however, is the fact that the trend towards improved tactile cue-integration on day 2 was most apparent when CC data was not considered. While corrections were done in our analysis to account for some issues that arose during the CC portion of the experiment, we cannot know to what extent our post hoc analysis is effective in eliminating error. Thus, at the moment, the non-conflict data is more informative to our final conclusions.

The pilot study aimed to examine the influence of extended training on participants' model choices, with three participants completing a 5-day experiment involving the same testing paradigm as the original study on days 1 and 5, but with days 2-4 only involving training on the non-conflict multi-stimulus piece. Preliminary results demonstrated varied effects on sensitivity and perceptual bias, but no general trend towards being particularly optimal. Bayesian analysis of posterior probabilities on days 1 and 5 suggested potential shifts in model classification.

While the pilot data suggests that cue combination within the hand perhaps reaches some threshold performance that is not improved relative to any individual digit, it would still be worthwhile to conduct the testing on a larger group of participants naive to the study to be certain of the effect of training on performance.

Another possible explanation for the less than optimal cue integration would

be that the cue combination task is somehow increasing the participant's cognitive load, in the sense that the brain is dividing its attention among the three digits, leading to each digit having a worse σ_s in the D234 condition. One of the key assumptions of our model is that the σ_s of each individual digit remains constant, but it could be that it becomes more difficult for the brain to accurately perceive the presentation of a cue with the additional digits present. One could also consider that under this assumption, the brain could in fact be combining the tactile cues optimally, but that each cue it receives is now less accurate. Further testing would be required to investigate whether this truly could be the case.

5.1 Sources of Error

In the course of our research, several potential sources of error and limitations have emerged, which necessitate a critical examination of the reliability and validity of our findings. These issues shed light on the complexity of the cue conflict paradigm and underscore the importance of refining our experimental design and analysis methods for future investigations.

5.1.1 Challenges in the Cue Conflict Paradigm

One significant challenge arose during the analysis of the cue conflict data. We observed an unexpected dip in the data, particularly on days 1 and 2, where participants displayed larger perceptual shifts than anticipated given the experimental conditions. Although we identified one potential source of this issue related to the width of the cue conflict stimulus piece, it is essential to acknowledge that there may be additional, as-yet undiscovered factors influencing these results. The complexity of the human sensory system and the intricacies of cue combination suggest that the true nature of sensory integration might involve more subtleties than currently understood.

5.1.2 Infinite Sub-Optimal Models

It is worth noting that there is a vast number of potential sub-optimal models, and the choice to include or exclude them in our analysis can significantly impact the

results. Our analysis hinges on the assumption that other possible models are non-significant in explaining participants' behavior. An example of this is the transition from considering three models to six models, highlighting the sensitivity of our conclusions to the model selection process. It remains an open question whether some of these other sub-optimal models could indeed contribute to explaining participants' responses to a certain extent, thus requiring further investigation.

5.1.3 Assumptions in our Analysis

Within our research framework, we rely on several assumptions that merit scrutiny. Firstly, the assumption of normality in modeling participants' perceptual biases and sensory acuity may not be entirely accurate, as individual variations in sensory processing can deviate from a strict normal distribution. Secondly, the assumption of independence between digits may not hold true in all scenarios, as the sensory system's interaction between adjacent digits could introduce dependencies. Moreover, the assumption that the brain inherently knows the acuity of each finger might not be entirely accurate, and participants might need to learn this information through specific training designed for the task. These assumptions highlight the need for future studies to consider alternative modeling approaches that accommodate these complexities.

5.1.4 Mechanical Considerations of Experiment

Another potential source of error that became evident during the study was the possibility of participants' fingers shifting from their initial location on the stimulus. This occurrence could influence participants' perception and create ambiguity in interpreting their sensory acuity. Also of note is the possibility that, after a certain number of trials, the cue pieces stability was slightly compromised as the screws would become loose over time to some small extent. This aspect, while not noticed in the original study, can be easily addressed by re-tightening the appropriate screws for future experiments. While these issues has been identified and addressed in subsequent studies by ensuring proper stimulus design, it is crucial to acknowledge its potential impact on our current data and thus our analysis.

5.1.5 Effect of Covid-19

The research conducted for this thesis was not without its share of challenges, many of which were exacerbated by the unique circumstances brought about by the Covid-19 pandemic. One significant obstacle was the strict limitations placed on in-person interactions and testing with study participants. The necessary safety measures and restrictions made it particularly challenging to conduct tactile perception experiments that required close physical proximity. Adhering to safety protocols, we found creative solutions to continue our research while ensuring the health and well-being of both participants and researchers. Moreover, the pandemic-induced limitations extended to collaboration with peers, with remote work and physical distancing measures impacting the free exchange of ideas and discussions amongst peers and collaborators. Despite these challenges, the dedication and adaptability of this research team allowed us to navigate these unprecedented circumstances and successfully conduct this study.

5.2 Future Directions

As we reflect on the outcomes and limitations of our current study, it becomes evident that there are promising avenues for future research that can both enhance our understanding of sensory integration and address some of the unresolved issues we encountered during this investigation.

5.2.1 Pilot Study Insights

Building on the insights gained from our pilot study, we recognize the need for further refinement in the design and execution of our experiments. One issue that we have yet to fully resolve is the occurrence of participants' digits landing on the wrong edges of the cue conflict stimulus. This unintended outcome could potentially skew our results and interpretations. However, we are committed to rectifying this issue in the forthcoming actual study by implementing more precise control measures to ensure that participants' fingers are appropriately positioned. Additionally, some participants in our pilot study exhibited a high degree of familiarity with the study and its premises, which could influence their responses.

Future investigations will aim to recruit participants who have no prior exposure to the study, reducing the potential for familiarity bias and enhancing the generalizability of our findings.

5.2.2 Manipulating Digit Acuity

Another intriguing avenue for future research involves artificially manipulating the sensory acuity of one specific digit, such as the index finger, and examining its impact on participants' behavior. By increasing the σ_s of the index finger's sensory estimate, we can create a controlled scenario to probe which model participants are using for sensory integration. If participants consistently prioritize information from the index finger, even when it is less reliable due to the increased sigma, it could provide valuable insights into their perceptual decision-making processes. This approach allows us to explore the robustness of the models under different conditions and gain a deeper understanding of how sensory uncertainty influences the integration of tactile information.

5.2.3 Broader Applications

Expanding upon our current study's outcomes and potential future directions, we hope that one day the insights gained here can extend beyond the realm of pure research. The principles and findings from our investigation into sensory integration and perceptual decision-making hold promise for various applications, particularly in the fields of robotics and surgery (Sankar et al., 2021).

In the field of robotics, our research can inform the development of tactile sensors and robotic systems that aim to mimic human-like tactile perception. By understanding how humans integrate sensory cues to make decisions, we can guide the creation of robots that interact more intuitively with their environments. These robots could possess improved object recognition capabilities and adaptability in various tasks, including those requiring dexterity and object manipulation. Such research would have particular relevance in the field of prosthetics, as those with impaired arms or hands would benefit from robotic limbs which can both act to manipulate objects *and* sense them.

Moreover, the knowledge derived from our study can be beneficial in surgical contexts. Surgeons rely heavily on haptic feedback during minimally invasive procedures Patel et al. (2022), where direct tactile contact is limited. Understanding how the human brain processes and integrates tactile information can lead to the design of more advanced haptic feedback systems for surgical robots. These systems could provide surgeons with enhanced tactile sensations, improving their ability to perform delicate and precise procedures.

By considering these potential applications in the fields of robotics and surgery, our research not only advances our fundamental understanding of sensory integration but also contributes to practical advancements in technology and healthcare. As we continue to explore and refine the intricacies of human tactile perception, we anticipate that these insights will play a pivotal role in shaping the future of these industries.

5.2.4 Conclusion

In conclusion, our research endeavor into the intricacies of sensory integration and perceptual decision-making has shed light on the multifaceted nature of human tactile perception. While our study has unveiled valuable insights and raised important questions, it also highlights the complexity of this phenomenon. As we navigate the intricate interplay between sensory modalities and decision processes, there remains much to explore, refine, and understand, with particular emphasis on the role of cue integration in the sensory system. With ongoing dedication to empirical rigor and innovative approaches, the path forward promises continued revelations and a deepening of our comprehension of how humans process and integrate sensory information.

Appendix A

Supplemental Derivations

Unweighted Average Model: σ_{234}

In our calculations each stimulus applied to a digit (D2, D3 and D4) produces a measurement distribution which is modelled as a Gaussian.

D234 will thus have a percept of $\mu_{234} = \frac{x_2+x_3+x_4}{3}$ under the AVG model (see Table 2.1), where each x_i indicates the cue percept of that stimulus applied to the respective digit. Beginning with $x = x_2 + x_3 + x_4$, we note that since the distributions are Gaussian, when adding the percept we can also add their variances.

$$\sigma_x^2 = \sigma_2^2 + \sigma_3^2 + \sigma_4^2 \tag{A.1}$$

$$\sigma_x = \sqrt{\sigma_2^2 + \sigma_3^2 + \sigma_4^2} \tag{A.2}$$

Since $\mu_{234} = \frac{x}{3}$, this means that $\sigma_{234} = \frac{\sigma_x}{3}$ as well.

$$\sigma_{234} = \frac{\sqrt{\sigma_2^2 + \sigma_3^2 + \sigma_4^2}}{3} \tag{A.3}$$

And thus the AVG model derivation of σ_{234} is complete.

Optimal Model: σ_{234}

If we examine the percept formula for the optimal model, as shown in Table 2.1 we can apply a similar logic to the AVG model to calculate σ_{234}. We start by keeping in mind our final equation of our percept, $\mu_{234} = \frac{\frac{x_2}{\sigma_2^2} + \frac{x_3}{\sigma_3^2} + \frac{x_4}{\sigma_4^2}}{\frac{1}{\sigma_2^2} + \frac{1}{\sigma_3^2} + \frac{1}{\sigma_4^2}}$. We know that each individual digit's percept, x_i will have a standard deviation of σ_i, and multiplying both sides by a constant will still maintain equality, as seen in equation A.4 for x_2.

$$sd\left(x_2 \cdot \frac{\frac{1}{\sigma_2^2}}{\frac{1}{\sigma_2^2} + \frac{1}{\sigma_3^2} + \frac{1}{\sigma_4^2}}\right) = \sigma_2 \cdot \left(\frac{\frac{1}{\sigma_2^2}}{\frac{1}{\sigma_2^2} + \frac{1}{\sigma_3^2} + \frac{1}{\sigma_4^2}}\right) = \frac{\frac{1}{\sigma_2}}{\frac{1}{\sigma_2^2} + \frac{1}{\sigma_3^2} + \frac{1}{\sigma_4^2}} \tag{A.4}$$

Since the variance of μ_{234} is the sum of the the variances of μ_2, μ_3 and μ_4, we will have the following result.

$$\sigma_{234}^2 = \sigma_2^2 + \sigma_3^2 + \sigma_4^2 \tag{A.5}$$

$$\sigma_{234}^2 = \left(\frac{\frac{1}{\sigma_2}}{\frac{1}{\sigma_2^2} + \frac{1}{\sigma_3^2} + \frac{1}{\sigma_4^2}}\right)^2 + \left(\frac{\frac{1}{\sigma_3}}{\frac{1}{\sigma_2^2} + \frac{1}{\sigma_3^2} + \frac{1}{\sigma_4^2}}\right)^2 + \left(\frac{\frac{1}{\sigma_4}}{\frac{1}{\sigma_2^2} + \frac{1}{\sigma_3^2} + \frac{1}{\sigma_4^2}}\right)^2 \tag{A.6}$$

$$\sigma_{234}^2 = \frac{\frac{1}{\sigma_2^2} + \frac{1}{\sigma_3^2} + \frac{1}{\sigma_4^2}}{\left(\frac{1}{\sigma_2^2} + \frac{1}{\sigma_3^2} + \frac{1}{\sigma_4^2}\right)^2} = \frac{1}{\frac{1}{\sigma_2^2} + \frac{1}{\sigma_3^2} + \frac{1}{\sigma_4^2}} \tag{A.7}$$

$$\sigma_{234} = \sqrt{\frac{1}{\frac{1}{\sigma_2^2} + \frac{1}{\sigma_3^2} + \frac{1}{\sigma_4^2}}} \tag{A.8}$$

Thus completing the derivation of σ_{234} under the OPT model.

Perceptual Shift Under Cue Conflict

As mentioned previously, the μ_{234} under the optimal model is $\mu_{234} = \frac{\frac{x_2}{\sigma_2^2} + \frac{x_3}{\sigma_3^2} + \frac{x_4}{\sigma_4^2}}{\frac{1}{\sigma_2^2} + \frac{1}{\sigma_3^2} + \frac{1}{\sigma_4^2}}$. Under the CC condition, however, we can more precisely state what each digit will be relative to the other. More specifically, $x_2 = \Delta + \delta$, $x_3 = \Delta$ and $x_4 = \Delta - \delta$ for $\delta = -1.0, -0.5, +0.5,$ or $+\,1.0$ mm.

Replacing these terms we find the following:

$$\mu_{234} = \frac{\frac{\Delta+\delta}{\sigma_2^2} + \frac{\Delta}{\sigma_3^2} + \frac{\Delta-\delta}{\sigma_4^2}}{\frac{1}{\sigma_2^2} + \frac{1}{\sigma_3^2} + \frac{1}{\sigma_4^2}} = \left(\frac{\frac{1}{\sigma_2^2} - \frac{1}{\sigma_4^2}}{\frac{1}{\sigma_2^2} + \frac{1}{\sigma_3^2} + \frac{1}{\sigma_4^2}} \right) \delta + \left(\frac{\frac{1}{\sigma_2^2} + \frac{1}{\sigma_3^2} + \frac{1}{\sigma_4^2}}{\frac{1}{\sigma_2^2} + \frac{1}{\sigma_3^2} + \frac{1}{\sigma_4^2}} \right) \Delta \tag{A.9}$$

$$\mu_{234} = \left(\frac{\frac{1}{\sigma_2^2} - \frac{1}{\sigma_4^2}}{\frac{1}{\sigma_2^2} + \frac{1}{\sigma_3^2} + \frac{1}{\sigma_4^2}} \right) \delta + \Delta \tag{A.10}$$

Thus, when comparing a reference CC edge to the location of the straight comparison edge (the latter edge being shifted by Δ on some trial), we would expect the perceived difference to be $\Delta + \left(\frac{\frac{1}{\sigma_2^2} - \frac{1}{\sigma_4^2}}{\frac{1}{\sigma_2^2} + \frac{1}{\sigma_3^2} + \frac{1}{\sigma_4^2}} \right) \delta$. Hence why the participant's psychometric function is now "biased" compared to a 2IFC task in which only straight edges are applied.

Bibliography

Alais, D., & Burr, D. (2004). The ventriloquist effect results from near-optimal bimodal integration. *Current Biology*, *14*, 257–262.

Bayes, T., Price, R., & Canton, J. (1763). An essay towards solving a problem in the doctrine of chances. by the late rev. mr. bayes, f. r. s. communicated by mr. price, in a letter to john canton, a. m. f. r. s. *Philosophical Transactions (1683-1775)*, *53*, 370–418.

Bialek, W., & Setayeshgar, S. (2005). Physical limits to biochemical signaling. *The Proceedings of the National Academy of Sciences*, *102*, 10040–10045.

Bruns, P. (2019). The ventriloquist illusion as a tool to study multisensory processing: An update. *Frontiers in Integrative Neuroscience*, *13*. https://doi.org/10.3389/fnint.2019.00051

Camponogara, I., & Volcic, R. (2021). Integration of haptics and vision in human multisensory grasping. *Cortex*, *135*, 173–185.

Dargahi, J., & Najarian, S. (2004). Human tactile perception as a standard for artificial tactile sensing–a review. *The International Journal of Medical Robotics + Computer Assisted Surgery : MRCAS*, *1*, 23–25.

Ernst, M. O., & Banks, M. S. (2002). Humans integrate visual and haptic information in a statistically optimal fashion. *Nature*, *415*, 429–433.

Faisal, A. A., Selen, L. P. J., & Wolpert, D. M. (2008). Noise in the nervous system. *Nature Reviews Neuroscience*, *9*, 292–303.

Frank, T. D., Friedrich, R., & Beek, P. J. (2006). Stochastic order parameter equation of isometric force production revealed by drift-diffusion estimates. *Phys. Rev. E*, *74*, 051905.

Ghahramani, Z. (1995). *Computational and psychophysics of sensorimotor integration* [Doctoral dissertation, Massachusetts Institute of Technology].

Green, D. M., & Swets, J. A. (1996). *Signal detection theory and psychophysics*. John Wiley & Sons.

Handler, A., & Ginty, D. D. (2021). The mechanosensory neurons of touch and their mechanisms of activation. *Nature Reviews Neuroscience*, *22*, 521–537.

Heeger, D. (1997). *Signal detection theory* (tech. rep.). New York University.

Jeffreys, H. (1961). *Theory of probability*. Oxford University Press.

Johansson, R. S., & Flanagan, J. R. (2009). Coding and use of tactile signals from the fingertips in object manipulation tasks. *Nature Reviews Neuroscience*, *10*, 345–359.

Johnson, K. 0. (2001). The roles and functions of cutaneous mechanoreceptors. *Current Opinion in Neurobiology*, *11*, 455–461.

Klein, S. A. (2001). Measuring, estimating, and understanding the psychometric function: A commentary. *Perception & Psychophysics*, *63*, 1421–1455.

Knill, D. C., & Pouget, A. (2004). The bayesian brain: The role of uncertainty in neural coding and computation. *Trends in Neuroscience*, *27*, 713–719.

Kontsevich, L. L., & Tyler, C. W. (1999). Bayesian adaptive estimation of psychometric slope and threshold. *Vision Research*, *39*, 2729–2737.

Körding, K. P., & Wolpert, D. M. (2004). Bayesian integration in sensorimotor learning. *letters to nature*, *427*, 244–248.

Luce, R. D., & Krumhansl, C. L. (1988). *Measurement, scaling, and psychophysics in r. c. atkinson, r. j. herrnstein, g. lindzey, & r. d. luce (eds.), stevens' handbook of experimental psychology: Perception and motivation; learning and cognition*. Oxford, UK: Wiley.

Macmillan, N. A., Hautus, M. J., & Creelman, C. D. (2022). *Detection theory a user's guide (third edition.)* Routledge.

McGurk, H., & MacDonald, J. (1976). Hearing lips and seeing voices. *Nature*, *264*, 746–748.

Merleau-Ponty, M. (1962). *Phenomenology of perception* (C. Smith, Trans.). Routledge.

Ostenfeld, E. (2018). *Ancient greek psychology and the modern mind-body debate, 2nd edition*. Baden-Baden, Germany: Academia Verlag, Baden-Baden.

Patel, R. V., Atashzar, S. F., & Tavakoli, M. (2022). Haptic feedback and force-based teleoperation in surgical robotics. *Proceedings of the IEEE*, *110*(7), 1012–1027.

Pek, J., & Van Zandt, T. (2020). Frequentist and bayesian approaches to data analysis: Evaluation and estimation. *Psychology Learning & Teaching*, *19*, 21–35.

Prodribaba, N. (2018). *An investigation of multiple-digit cue combination: Psychophysics and bayesian modelling.*

Riemer, M., Trojan, J., Beauchamp, M., & Fuchs, X. (2019). The rubber hand universe: On the impact of methodological differences in the rubber hand illusion. *Neuroscience & Biobehavioral Reviews*, *104*, 268–280.

Rohe, T., & Noppeney, U. (2015). Cortical hierarchies perform bayesian causal inference in multisensory perception. *PLoS Biol*, *13*.

Rosas, P., Wagemans, J., Ernst, M. O., & Wichmann, F. A. (2005). Texture and haptic cues in slant discrimination: Reliability-based cue weighting without statistically optimal cue combination. *J. Opt. Soc. Am. A*, *22*, 801–809.

Sankar, S., Balamurugan, D., Brown, A., Ding, K., Xu, X., Low, J. H., Yeow, C. H., & Thakor, N. (2021). Texture discrimination with a soft biomimetic finger using a flexible neuromorphic tactile sensor array that provides sensory feedback. *Soft Robotics*, *8*, 577–587.

Sathian, K., Lacey, S., Stilla, R., Gibson, G. O., Deshpande, G., Hu, X., LaConte, S., & Glielmi, C. (2011). Dual pathways for haptic and visual perception of spatial and texture information. *NeuroImage*, *57*, 462–475.

Tanner Jr., W. P., & Swets, J. A. (1954). A decision-making theory of visual detection. *Psychological Review*, *61*(6), 401–409.

Tolhurst, D., Movshon, J., & Dean, A. (1983). The statistical reliability of signals in single neurons in cat and monkey visual cortex. *Vision Res.*, *23*, 775–785.

Treisman, M., & Faulkner, A. (1985). On the choice between choice theory and signal detection theory. *The Quarterly Journal of Experimental Psychology Section A*, *37*, 387–405.

Wickens, T. (2002). *Elementary signal detection theory.* Oxford University Press.

Wixted, J. T. (2020). The forgotten history of signal detection theory. *Journal of Experimental Psychology: Learning, Memory, and Cognition*, *46*, 201–233.

Zuidhoek, S., Visser, A., Bredero, M., & Postma, A. (2004). Multisensory integration mechanisms in haptic space perception. *Exp Brain Res*, *157*, 265–268.